IEEE Access
Multidisciplinary | Rapid Review | Open Access Journal

Received February 20, 2020, accepted March 10, 2020, date of publication March 30, 2020, date of current version May 8, 2020.

Digital Object Identifier 10.1109/ACCESS.2020.2982028

A Time Fractional Model With Non-Singular Kernel the Generalized Couette Flow of Couple Stress Nanofluid

MUHAMMAD ARIF[1], FARHAD ALI[2,3], ILYAS KHAN[4], AND KOTTAKKARAN SOOPPY NISAR[5]

[1]Department of Mathematics, City University of Science and Information Technology, Peshawar, Khyber Pakhtunkhwa, Pakistan.
[2]Computational Analysis Research Group, Ton Duc Thang University, Ho Chi Minh City, Vietnam.
[3]Faculty of Mathematics and Statistics, Ton Duc Thang University, Ho Chi Minh City, Vietnam.
[4]Department of Mathematics, College of Science Al-Zulfi, Majmaah University, Al-Majmaah 11952, Saudi Arabia.
[5]Department of Mathematics, College of Arts and Science, Prince Sattam bin Abdulaziz University, Wadi Al-Dawaser 11991, Saudi Arabia.

Corresponding author: Farhad Ali (farhad.ali@tdtu.edu.vn)

ABSTRACT The aim of the present work is to calculate the closed form solutions of the unsteady couple stress nanofluids flow in a channel. Couple stress nanofluids (CSNF) is allowed to pass through the parallel plates separated by a distance h. In this study, we choose blood as base fluid with gold nanoparticles suspension. The lower plate is at rest and the upper plate is suddenly moved with constant velocity U_0. Recently, Atangana–Baleanu (AB) introduced a new definition of fractional derivatives. This AB definition of fractional derivative has been applied to the present couple stress nanofluid (CSNF) model. The closed form solutions of present CSNF model via AB approach are obtained by using the Laplace and finite Fourier sine transforms. Exact results of velocity and temperature are displayed and discussed for different parameters of interest. Solutions obtained here are reduced to three different cases in limiting sense i.e. (i) fractional couple stress nanofluid without external pressure gradient. (ii) ordinary couple stress nanofluid. (iii) regular couple stress fluid. Finally, skin friction and Nusselt number are evaluated at lower and upper plates and listed in tabular forms. The results show that increasing external pressure gradient, CSNF velocity increases whereas decreases by increasing Reynolds number. Increasing volume fraction slow down the CSNF velocity. The velocity of Newtonian viscous fluid is higher than CSNF velocity.

INDEX TERMS Couple stress nanofluid (gold in blood), Atangana–Baleanu, generalized Couette flow, Laplace and Fourier transforms.

NOMENCLATURE

CSNF	Couple Stress nanofluid
AB	Atangana–Baleanu
Au	Gold nanoparticles
ρ	Density
$\overrightarrow{V}$	Velocity in vector form
u	Velocity
w	Dimensionless velocity
T	Temperature
T_w	Wall temperature
T_h	Ambient temprature
β_T	Thermal expansion
k	Thermal conductivity
μ	Dynamic viscosity
c_p	Specific heat at constant pressure
g	Acceleration due to gravity
p	Pressure
b_1	Body forces
η	Couple stress parameter
h	Distance between the plates
U_0	Unifotm velocity
$H(t)$	Heaviside unit Step Function
Re	Reynolds number
Gr	Grashof number
Pr	Prandtl number
ϕ	Volume fraction of nano-particles
θ	Dimensionless temprature
G	Constant pressure gradient
τ	Time
${}^{AB}D_{\tau}^{\beta}$	Atangana–Baleanu fractional derivative
β	Fractional parameter

The associate editor coordinating the review of this manuscript and approving it for publication was Rosario Pecora.

This work is licensed under a Creative Commons Attribution 4.0 License. For more information, see https://creativecommons.org/licenses/by/4.0/

E_β	Expression for Mittag-Leffler function
$F_\alpha(.,.)$	Expression of Robotnov and Hartleys' function
$w_p(\xi)$	Steady velocity field
$w_\tau(\xi,\tau)$	Unsteady Velocity field
$Sf(\xi,t)\,Nu$	Skin friction Nusselt number
$Sf(0,t)$	Skin friction at lower plate
$Sf(1,t)$	Skin friction at upper plate

I. INTRODUCTION

There are many kind of fluids in nature one is Newtonian and the other one are non-Newtonian fluids which have a lot of industrial and daily life applications in many physical, practical and different engineering processes. Non-Newtonian fluids have widely used for engineering and practical life applications puroses. Due to this popularity of non-Newtonian fluids, recently researchers are more interested to study these fluids. Couple stress fluid (CSF) is considered as non-Newtonian fluid which is less investigated in the recent literature. The idea of CSF theory was discovered by Stokes [1]. He noticed that couple stresses are the simplest generalization theory of the classical fluids which allows for the effect of polar such as the presence of couple stress forces and body couples. In another paper the theory related to CSF is investigated briefly by Stokes [2]. In this paper he also shows the applications of CSF and different real world problems which are calculated by many researchers.

Couple stress fluids (CSFs) model have widely used in modern sciences and technology like, the crude oil is extraction phenomana, some applications in electrical engineering processes, the process of aerodynamics heating, solidification processes of liquid crystals, cooling processes of metallic plate in a bath, colloidal and suspension solutions [3]–[5]. The problems related to couple stress fluids (CSFs) in a channel have useful engineering and industrial applications.

CSF theory and mathematical model have many daily life applications, like pumping phenomena when the fluids synthesis lubricants and problems related to biological process and animal blood and many other example. The model of couple stress fluids have been chosen by scientists and researchers for many scientific and industrial uses which is applied on some physical real wolrd problems. Ramanaiah [6] discussed the siginificance of CSFs and use these fluids in different problems. Sinha and Singh [7] studied CSF for mechanical purposes like process of rolling contact bearings considering cavitation. Lin [8] explained the influences of couple stresses (CSs) and the characteristics of(CSs) inside the cyclic squeeze films and the advance characteristics of CSF between a sphere and a flat plate. Banyal [9] discussed the imporatant condition for the onset of stationary CSF. Devakar *et al.* [10] investigated CSF solutions of some fully developed flows inside the concentric cylinders the condition at the boundary is chosen as slip boundary conditions. In another paper Devakar and Iyengar [11] calcultated some CSF taking three different cases namely, CSF Couette flow, CSF Poiseuille and CSF generalized Couette flow. Furthermore, the conditions are taken in this study are slip boundary condition.

Opanuga *et al.* [12] investigated magnetohydrodynamics flow of CSFs using second law analysis. Khan *et al.* [13] calculated the closed form solutions for MHD flow of CSFs with the effect of heat transfer. Hayat *et al.* [14] discussed three-dimensional couple stress fluid flow over a stretched surface. Morever, there are many other analytical solutions couple stress fluid which have been analyzed by Naeem [15], a class of flows for CSFs. Beg *et al.* [16] investigated the mathematical modeling of oscillatory couple-stress bio-fluid in a rotating channel. CSFs have enormous applications in diverse fields of sciences like engnineering biological science and modern science. Due to these applications many researchers taking interest in CSFs and investigated for different scientific reasons and purposes. Like Adesanya and Makinde [17] showed the effects of CSF on entropy generations rate by cosidereing porous media and CSFs are considerd in a channel with convecting heating. In another article Adesanya and Makinde [18] calculated the process of irreversibility in a CSF flow with the effect of heated plate and adiabatic free surface. Furthermore, Naduvinamani *et al.* [19] investigated the effect of roughness of surface on couple stress squeeze film between anisotropic porous rectangular plates. Lin and Hung [20] discussed the combined effect of non-Newtonian CSFs inertia on the squeeze film characteristics between a long cylinder and an infinite plate. Lu and Lin [21] studied combinedly the effects of non-Newtonian rheology and viscosity-pressure system. Ashmawy [22] analyzed unsteady Couette flow of a micropolar fluid with slip effect.

There were some real world problems which cannot explained by simple classical models. To find the solutions of such problem fractional calculus was introduced. It means that fractional clculus is the generalized form of classical models. The idea of fractional calculus was developed when Leibniz gave the nth order derivatives representation of a function. Leibniz asked a question from Del Hospital that what will happen if we take the order of a differential equation in fraction. After that, many researchers start thinking over it and they introduced various definitions of fractional derivatives for many reasons. The researchers and scientists are carried their studies in fractional calculus due to the enormous very interesting useful applications in many fields of sciences especially in physical science, chemical science, science related to biology or living organisms, different fields of engineering and other sciences which have been grown up recently. The idea of fractional calculus used by many researchers initially which are mentioned in [23]. Furthermore, some useful applications of Fractional calculus (FC) in industries and engineering phenomena, for example, diffusion phenomena, dispersion and advection phenomena of different solutes in porous or fractured media [24]. Olmstead and Handelsman [25] investigated diffusion process. In this process thay explained a semi-infinite region by taking some nonlinear surfaces. In another paper

Marks and Hall [26] analyzed the differintegral interpolation phenomena from a bandlimited signal's samples. Cuesta *et al.* [27] also discussed the phenomenon of image denoising by using some generalized fractional models of time integrals. Similarly, Fareed *et al.* [28] explained some viscoelastic behavior of different materials briefly using the concept of fractional calculus. Gaul *et al.* [29] developed a fractional model for the purpose damping description phenomenon using the idea of fractional operators and definitions. Podlubny [30] explained some important applications regarding to fractional derivatives for the measurement of heat and load intensity by change in the blast furnace walls. The above are some useful applications in of fractional calculus in daily life in the field of engineering, some biological uses of fractional operators have been investigated by Magin [31]. Furthermore, the new fractional operators have a very strong and complex memories allowing capturing behaviors of combining simultaneously classical diffusions and anomalous behavior. Morever, the definitions of fractional derivative explained the viscoelastic and viscoplastic behavior of different materials. Due to these practical life applications like, Bio-engineering, kinetics of polymers and in many other areas of modern science and technologies the scientists are focused to discussed different phenomena using fractional calculus and fractional operators.

Based on the interest of researchers, several definitions for fractional derivatives have been proposed in the literature. Among them, Caputo-Fabrizio (CF) developed a fractional order derivatives on the basis of an exponential function, to remove the diffiecincy and shotcomings of singularity problem of the kernel in earlier studies [32]. Caputo-Fabrizio developed a fractional model which have no singular kernel. Recently, this fractional order definition is very famous in modern research in the field of fractional calculus. Due to this popularity many researchers have been chosen the definition of CF for various purposes in modern science to analyzed many problems. The definition of CF has non-locality problem to remove these deficiencies of non-locality of the kernel, a new definition has been developed by Atangana and Nieto [33] and Atangana [34] proposed a latest version of fractional derivatives definition which have no singularity and non-locality issues in their definition. This definition is new and very less investigation have been done using AB derivatives. This latest idea of AB fractional derivatives have been used by Arif *et al* [35] and for the sake of comparison CF fractional derivatives is also applied on the proposed problem. Furthermore, in this study they find the closed form solutions of very famous model couple stress fluid model in a channel taking the effect of external pressure gradient. Akhtar [36] also calculated the closed form solutions CSF in channel but they used Caputo and CF fractional model.

Research on nanofluids is getting more attention from the researchers these days due to several engineering and industrial application. A fluid consists of nanoparticles called nanofluid. Nanofluid formed by adding some nano-meter sized particles in the base fluids like water, kerosin oil, engine oil, transformer oil and many other fluids for the porpose of heat transfer enhancement. By the addition of these nanometer szed particles there is an increase occur in the rate of thermal conductivity which is the need of modern world. The size of these nanoparticles are (1-100) nanometer which dissolved in the base fluid forming nanofluids. It can be observed that the addition of these nanoparticles in the base fluid not only used for the enhancement of the thermal conductivity fluid but it also change the characteristcs and properties of the base fluid for many scientific purposes, when required. The first experimental work on nanofluid was conducted by Choi and Eastman [37] where he suspended nanometer-sized particles in conventional base fluids. Soon after, Choi work on this idea was used by other researchers for heat transfer enhancement, where they dispersed nanoparticles in base fluids. In fluid studies, the idea of nanoparticles in different base fluid was used by several researchers (for Newtonian fluids and non-Newtonian), however, for Couple stress fluids CSFs only a few studies exists. Ramzan [38] calculated some applications and effect of viscous dissipation and joule heating for CSF taking nanoparticles in their studies. Hayat *et al* [39] investigated the effect of magnetic field in 3D couple stress fluid flow inside arteries using the concept of nanoparticles. Arif *et al* [40] studied enhanced heat transfer in working fluids using nanoparticles with ramped wall temperature. Awais *et al* [41] discussed hydromagnetic effect on CSNF flow over a moving wall. As nanofluids are used in a wide range for different purposes in modern world. Recently, many researchers work on nanofluid and use these fluid in different circumstances like, Gireesha *et al.* [42], [43] investigated heat and mass transfer phenomena in chemically reacting Casson nanofluid model. Mahanthesh and Gireesha [44] explained thermal radiation, viscous dissipation and Joule heating effects on Marangoni convective two-phase flow of Casson fluid with fluid-particle suspension. In another paper Mahanthesh *et al.* [4] discussed the effect of Nonlinear radiative flow of casson nanoliquid which allow to past through a cone and wedge with magnetic dipole. Ramesh [45] explained the effect of heat and mass transfer on CSF fluid flow porous medium is also considered in this study with the effect of magnetic field in an inclined asymmetric channel. Different nanoparticles are used for various scientific reasons and engineering and biological purposes.

Blood is very important and necessary fluid in the human body and the motion of blood is explained by the biomagnetic fluid dynamics (BFD). In human body the the motion of blood can be described by hemodynamics. BFD examine the motion of the blood through vessels. As blood is the suspension of red blood cells in plasma, and it is in the category of non-Newtonian fluid. In the present study we have considered blood as base fluid and gold is chosen as nanoparticles. Many researchers have been used gold nanoparticles in blood base fluid for diferrent biological purposes.

The purpose of this article is to investigate unsteady couple stress nanofluid CSNF between the two parallel plates.

Additionally, blood is chosen as base fluid and gold (Au) nanoparticles are uniformly dispersed in the base fluid. Instead of the classical model of couple stress fluid, a time fractional model based on AB definition has been used. The Laplace transform and Fourier sine transform technique has been used to obtain the exact solutions for the present problem. The effects of various parameters are investigated on the fluid flow using different graphs. Finally, Skin fraction for (CSNF) for the lower and upper plate are calculated and presented the numerical values in tabular form.

II. MATHEMATICAL MODELING AND SOLUTION OF THE PROBLEM

The present study explained the flow behavior of laminar flow and an incompressible couple stress nanofluid (CSNF) have been taken inside an infinite horizontal channel between the two infinite parallel plates. The motion of blood base nanofluid is taken along the x -direction in the absence of body couples. The continuity and momentum equation of the CSNF and energy equation, are given by [46], [47]:

$$\nabla \cdot \vec{V} = 0, \tag{1}$$

$$\rho_{nf}\frac{\partial \vec{V}}{\partial t} = -\nabla p - \mu_{nf}\nabla \times \nabla \times \vec{V} - \eta \nabla \times \nabla \times \nabla \times \nabla \times \vec{V} + g\left(\rho\beta\right)_{nf}\left(T - T_{\infty}\right) + \rho\vec{b_1}, \tag{2}$$

$$\left(\rho c_p\right)_{nf}\frac{\partial T}{\partial t} = k_{nf}\nabla \times \nabla \times T. \tag{3}$$

Here ρ_{nf}, $\vec{V}$, T, $\vec{b_1}$, p, μ_{nf}, η, $\left(\rho c_p\right)_{nf}$ and k_{nf} represents density, velocity vector, temperature, body force vector, pressure, dynamic viscosity, couple stress parameter, heat capacitance of the nanofluid and thermal conductivity of the nanofluid. The velocity field for the present flow is $\vec{V} = (u(y,t), 0, 0)$ and temperature field is $T = (T(y,t), 0, 0)$ which satisfies all the equation of continuity (1) and the governing equations (2) and (3) of the CSNF and the body forces $\vec{b_1}$ is ignored in the present study [48]:

$$\rho_{nf}\frac{\partial u(y,t)}{\partial t} = -\frac{\partial p}{\partial x} + \mu_{nf}\frac{\partial^2 u(y,t)}{\partial y^2} - \eta\frac{\partial^4 u(y,t)}{\partial y^4} + g\left(\rho\beta\right)_{nf}\left(T - T_{\infty}\right), \tag{4}$$

$$\left(\rho c_p\right)_{nf}\frac{\partial T(y,t)}{\partial t} = k_{nf}\frac{\partial^2 y(y,t)}{\partial y^2}. \tag{5}$$

1) GENERALIZED COUETTE FLOW

The flow between the plates in which one plate is stationary and second plate is moving with constant velocity with the effect of external pressure gradient such type of fluid motion is called generalized Couette flow.

The CSNF fluid between the plates is incompressible, laminar and plates are separated by a distance h. In this problem upper plate is stationary and the lower plate is assumed to have a constant velocity U_0. The lower plate temperature is T_w and the upper plate has an ambient temperature T_h. In the given work gold (Au) is taken in blood as base fluid. Additionally, the CSNF motion is along the x -direction due to the constant pressure gradient G as shown in Fig. 1.

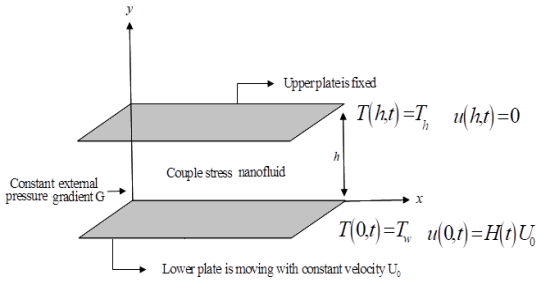

FIGURE 1. Geometry of the problem.

According to the above assumptions, the governing equations along with initial and boundary conditions are given as [36], [48]:

$$\rho_{nf}\frac{\partial u(y,t)}{\partial t} = G^* + \mu_{nf}\frac{\partial^2 u(y,t)}{\partial y^2} - \eta\frac{\partial^4 u(y,t)}{\partial y^4} + g\left(\rho\beta_T\right)_{nf}\left(T - T_{\infty}\right), \tag{6}$$

$$\left(\rho c_p\right)_{nf}\frac{\partial T(y,t)}{\partial t} = k_{nf}\frac{\partial^2 y(y,t)}{\partial y^2}, \tag{7}$$

$$\left.\begin{array}{l} u(y,0) = 0, \quad T(y,0) = 0, \text{ for } 0 \le y \le h \\ u(0,t) = H(t)U_0, \quad T(0,t) = T_w, \text{ for } t > 0, \\ u(h,t) = 0, \quad T(h,t) = T_h, \quad \text{for } t > 0, \\ \dfrac{\partial^2 u(0,t)}{\partial y^2} = \dfrac{\partial^2 u(h,t)}{\partial y^2} = 0, \quad \text{for } t > 0, \end{array}\right\} \tag{8}$$

where $H(t)$ represents Heaviside function.

For nanofluids, the expressions of ρ_{nf}, μ_{nf}, $\left(\rho c_p\right)_{nf}$, $\left(\rho\beta_T\right)_{nf}$ and k_{nf} are given by [48].

$$\rho_{nf} = \rho_f\left((1-\phi) + \frac{\phi\rho_s}{\rho_f}\right), \quad \mu_{nf} = \mu_f\left(\frac{1}{(1-\phi)^{2.5}}\right),$$
$$\left(\rho\beta_T\right)_{nf} = \left(\rho\beta_T\right)_f\left[(1-\phi) + \frac{\phi\left(\rho\beta_T\right)_s}{\left(\rho\beta_T\right)_f}\right],$$
$$k_{nf} = k_f\left[\frac{2k_f + k_s - 2\phi(k_f - k_s)}{2k_f + k_s + \phi(k_f - k_s)}\right],$$
$$\left(\rho c_p\right)_{nf} = \left(\rho c_p\right)_f\left[(1-\phi) + \frac{\phi\left(\rho c_p\right)_s}{\left(\rho c_p\right)_f}\right]. \tag{9}$$

Here ρ_f and ρ_s represents the density of the base fluid and solid particles respectively, μ_f and μ_s represents the dynamic viscosity of the base fluid and solid particles respectively, k_f and k_s represents thermal conductivity of the base fluid solid particles respectively.

The following non-dimensional quantities have been used for dimensional analysis.

$$\xi = \frac{y}{h}; \quad w = \frac{u}{U_0}; \quad \tau = \frac{U_0 t}{h}, \quad \theta = \frac{T - T_h}{T_w - T_h}.$$

TABLE 1. Thermo-physical properties of Blood and Gold nanoparticles [48], [49].

Material	Blood	Gold
Symbol	-	Au
$\rho\left(Kgm^{-3}\right)$	1050	19300
$c_p\left(JKg^{-1}K^{-1}\right)$	3617	129
$k\left(Wm^{-1}K^{-1}\right)$	0.52	318

into equations(6-8), we get:

$$A\frac{\partial w(\xi,\tau)}{\partial \tau} = G + \frac{\partial^2 w(\xi,\tau)}{\partial \xi^2} - \lambda\frac{\partial^4 w(\xi,\tau)}{\partial \xi^4} + B\theta\,(\xi,\tau)\,, \tag{10}$$

$$P_0\frac{\partial \theta(y,\tau)}{\partial \tau} = \frac{\partial^2 \theta(\xi,\tau)}{\partial \xi^2}, \tag{11}$$

$$\left.\begin{array}{l} w=0,\theta=0, \text{ for } 0\le\xi\le 1 \text{ and } \tau=0,\\ w=1,\theta=1, \text{ for } \xi=0 \text{ and } \tau>0,\\ w=0,\theta=0, \text{ for } \xi=1 \text{ and } \tau>0,\\ \dfrac{\partial^2 w}{\partial \xi^2}=0, \text{at } \xi=0 \text{ and } \xi=1. \end{array}\right\}. \tag{12}$$

Here $a_0 = (1-\phi)^{2.5}$,

$$a_1 = (1-\phi)+\phi\frac{\rho_s}{\rho_f},$$
$$a_2 = (1-\phi)+\phi\frac{(\rho\beta_T)_s}{(\rho\beta_T)_f},$$
$$b_0 = (1-\phi)+\phi\frac{(\rho c_p)_s}{(\rho c_p)_f},$$
$$b_0 = (1-\phi)+\phi\frac{(\rho c_p)_s}{(\rho c_p)_f},$$
$$b_1 = \frac{(k_s+2k_f)-2\phi(k_f-k_s)}{(k_s+2k_f)+\phi(k_f-k_s)},$$
$$P_0 = \frac{\mathrm{Pr}\,hb_0U_0}{\nu_f b_1}, A = \mathrm{Re}\,a_0a_1,$$
$$B = Gra_0a_2, \mathrm{Re} = \frac{U_0h}{\nu_f},$$
$$\mathrm{Pr} = \frac{\mu c_p}{k_f}, Gr = \frac{h^2g\beta\,(T_w-T_\infty)}{\upsilon_f U_0},$$
$$G = \frac{G^*a_0h^2}{\mu_f U_0}, \lambda = \frac{a_0\eta}{\mu_f h^2}.$$

where Re, Pr, Gr, G, G^* and λ represents the Reynolds number, Prandtl number, Grashof number, pressure gradient, dimensional pressure and nanofluid particles size effect due to Couple stresses respectively.

III. EXACT SOLUTIONS USING ATANGANA-BALEANU FRACTIONAL DERIVATIVES

Applying the definition of Atangana-Baleanu to the governing equations we get the following fractional CSNF model with fractional operator β as follows:

$${}^{AB}\mathbf{D}_\tau^\beta Aw(\xi,\tau) = G + \frac{\partial^2 w(\xi,\tau)}{\partial \xi^2} - \lambda\frac{\partial^4 w(\xi,\tau)}{\partial \xi^4} + B\theta\,(\xi,\tau)\,, \tag{13}$$

$${}^{AB}\mathbf{D}_\tau^\beta P_0\theta(\xi,\tau) = \frac{\partial^2 \theta(\xi,\tau)}{\partial \xi^2}. \tag{14}$$

Here ${}^{AB}\mathbf{D}_\tau^\beta$ is the definition of AB time-fractional derivatives having order β which is defined as [34].

$${}^{AB}\mathbf{D}_\tau^\beta(\tau) = \frac{N(\beta)}{(1-\beta)}\int_0^\tau E_\beta\left(\frac{-\beta\,(\tau-t)^\beta}{1-\beta}\right)f'(\tau)\,dt, \tag{15}$$

where $N(\beta)$ represents here normalization function, such that $N(1) = N(0) = 1$ and $\beta \in (0,1)$.

In Eq (15) E_β shows the generalized Mittag-Leffler function defined by [50].

$$E_\beta\left(-t^\beta\right) = \sum_{k=0}^{\infty}\frac{(-t)^{\beta k}}{\Gamma(\beta k+1)}. \tag{16}$$

A. SOLUTIONS OF ENERGY EQUATION

The Laplace transform technique is applied to Eq. (14) and incorporate the initial condition which is given in Eq. (12), we have the following transform equation:

$$\frac{p^\beta P_0H_1\overline{\theta}\,(\xi,p)}{\left(p^\beta+H_2\right)} = \frac{d^2\overline{\theta}\,(\xi,p)}{d\xi^2}, \tag{17}$$

After applying the Laplace transform to boundary conditions Eq. (12) reduces to the following form:

$$\left.\begin{array}{l} \overline{w}\,(\xi,p)=\dfrac{1}{q}\,,\ \overline{\theta}\,(\xi,p)=\dfrac{1}{p}\text{for } \xi=0 \text{ and} p>0,\\ \overline{w}\,(\xi,p)=0,\ \overline{\theta}\,(\xi,p)=0, \text{for } \xi=1 \text{and } p>0,\\ \dfrac{\partial^2\overline{w}\,(\xi,p)}{\partial\xi^2}=0, \text{at } \xi=0 \text{ and } \xi=1. \end{array}\right\} \tag{18}$$

Applying the sine Fourier transform to Eq. (17) taking the limits from 0 to h with respect to ξ and incorporate Eq. (18), we obtained the following solution:

$$\overline{\theta}_s\,(n,p) = \frac{\sigma_n}{p}\left(\frac{\left(p^\beta+H_2\right)}{H_1P_0p^\beta+\sigma_n\left(p^\beta+H_2\right)}\right), \tag{19}$$

equivalently,

$$\overline{\theta}_s\,(n,p) = \left(\frac{H_3\left(p^\beta+H_2\right)}{p\left(p^\beta+H_4\right)}\right). \tag{20}$$

Applying partial fraction, we get the following result:

$$\overline{\theta}_s(n,p) = \frac{H_3H_2}{H_4p} + \frac{H_3(H_4-H_2)}{H_4}\frac{1}{p^{1-\beta}\left(p^\beta+H_4\right)}. \tag{21}$$

The inverse Laplace result:

$$\theta_s(n,\tau) = \frac{H_3H_2}{H_4} + \frac{H_3(H_4-H_2)}{H_4}h(t) * F_\beta(-H_4,\tau), \tag{22}$$

where

$$F_\beta(-H_4,\tau) = L^{-1}\left(\frac{1}{p^\beta+H_4}\right) = \sum_{n=0}^{\infty}\frac{(-H_4)^n\tau^{(n+1)\beta-1}}{\Gamma((n+1)\beta)}. \tag{23}$$

Here $F_\alpha(.,.)$ shows robotnov and Hartleys' function which is defined in [51]. Moreover,

$$L^{-1}\left(\frac{1}{s^{1-\beta}}\right) = h(t) = \frac{1}{t^\beta\Gamma(1-\beta)}$$
$$H_1 = 1/1-\beta, \sigma_n = n\pi/h, H_2 = \beta/1-\beta,$$
$$H_3 = \frac{\sigma_n}{H_1P_0+\sigma_n^2}, \text{ and } H_4 = \frac{\sigma_n^2H_2}{H_1P_0+\sigma_n^2}.$$

By using inverse sine-Fourier transform to Eq. (22), we have the following form [52], [53].

$$\theta(\xi,\tau) = 1 - \frac{\xi}{h} - \left(\frac{\xi(h-1)}{h}\right) + \frac{2}{h}\sum_{n=1}^{\infty}\frac{H_3(H_4-H_2)}{H_4}h(t) * F_\beta(-H_4,\tau)\sin\left(\frac{n\pi\xi}{h}\right). \tag{24}$$

B. SOLUTIONS OF MOMENTUM EQUATION

The Laplace transform is applied to Eq. (13) and initial condition which is given in Eq. (12), have been incorporated the following solutions are obtained:

$$\frac{AH_1p^\beta}{p^\beta+H_2}\overline{w}(\xi,p) = \frac{G}{p} + \frac{d^2\overline{w}(\xi,p)}{d\xi^2} - \lambda\frac{d^4\overline{w}(\xi,p)}{d\xi^4} + B\overline{\theta}(\xi,p). \tag{25}$$

Apply the sine Fourier transform to Eq. (25) and taking limits from 0 to h with respect to ξ and using Eq. (18), we have the following solution:

$$\frac{AH_1p^\beta}{p^\beta+H_2}\overline{w}_s(n,p) = \frac{G(1-(-1)^n)}{p\sigma_n} + \frac{\sigma_n}{p} - \sigma_n^2\overline{w}_s(n,p) + \lambda\frac{\sigma_n^3}{p} - \lambda\sigma_n^4\overline{w}_s(n,p) + B\overline{\theta}_s(n,p). \tag{26}$$

Multiply $\frac{p^\beta+H_2}{AH_1p^\beta}$ both sides, we get:

$$\overline{w}_s(n,p) = \left(\frac{G(1-(-1)^n)+\sigma_n^2+\lambda\sigma_n^4}{p\sigma_n}\right) \times \left[\frac{\left(p^\beta+H_2\right)}{\left(AH_1p^\beta+\sigma_n^2\left(p^\beta+H_2\right)+\lambda\sigma_n^4\left(p^\beta+H_2\right)\right)}\right] + B\overline{\theta}_s(n,p) \times \left[\frac{\left(p^\beta+H_2\right)}{\left(AH_1p^\beta+\sigma_n^2\left(p^\beta+H_2\right)+\lambda\sigma_n^4\left(p^\beta+H_2\right)\right)}\right]. \tag{27}$$

Equation (27) in more appropriate form can be written as:

$$\overline{w}_s(n,p) = \left(\frac{G(1-(-1)^n)+\sigma_n^2+\lambda\sigma_n^4}{p\sigma_n}\right) \times \left[\frac{H_5\left(p^\beta+H_2\right)}{\left(p^\beta+H_6\right)}\right] + B\overline{\theta}_s(n,p) \times \left[\frac{H_5\left(p^\beta+H_2\right)}{\left(p^\beta+H_6\right)}\right], \tag{28}$$

where,

$$H_5 = \frac{1}{AH_1+\sigma_n^2+\lambda\sigma_n^4},$$
$$H_6 = \frac{\sigma_n^2H_2+\lambda\sigma_n^4H_2}{AH_1+\sigma_n^2+\lambda\sigma_n^4}.$$

Substituting, $\overline{\theta}_s(n,p)$ from Eq. (20) into equation (28), we get:

$$\overline{w}_s(n,p) = H_5\left(\frac{G(1-(-1)^n)+\sigma_n^2+\lambda\sigma_n^4}{\sigma_n}\right) \times \left[\frac{\left(p^\beta+H_2\right)}{p\left(p^\beta+H_6\right)}\right] + BH_3H_5\left(\frac{\left(p^\beta+H_2\right)}{p\left(p^\beta+H_4\right)}\right) \times \left[\frac{\left(p^\beta+H_2\right)}{\left(p^\beta+H_6\right)}\right]. \tag{29}$$

Separation of the RHS of Eq. (29) using partial fraction gives:

$$\overline{w}_s(n,p) = \left(\frac{G(1-(-1)^n)+\sigma_n^2+\lambda\sigma_n^4}{\sigma_n}\right) \times \left(\frac{H_5H_2}{H_6p} + \frac{H_5(H_6-H_2)}{H_6p^{1-\beta}\left(p^\beta+H_6\right)}\right) + BH_3H_5\left[\begin{array}{l}\frac{1}{p} - \frac{(H_2-H_4)^2}{(H_4-H_6)p\left(p^\beta+H_4\right)} \\ + \frac{(H_2-H_6)^2}{(H_4-H_6)p\left(p^\beta+H_6\right)}\end{array}\right]. \tag{30}$$

Taking the inverse Laplace transform we obtain the following solution:

$$w_s(n,\tau) = \left(\frac{G(1-(-1)^n)+\sigma_n^2+\lambda\sigma_n^4}{\sigma_n}\right) \times \left(\frac{H_5H_2}{H_6} + \frac{H_5(H_6-H_2)}{H_6}h(t) * F_\beta(-H_6,\tau)\right) + BH_3H_5\left[\begin{array}{l}1 - \frac{(H_2-H_4)^2}{(H_4-H_6)}1 * F_\beta(-H_4,\tau) \\ + \frac{(H_2-H_6)^2}{(H_4-H_6)}1 * F_\beta(-H_6,\tau)\end{array}\right], \tag{31}$$

where

$$L^{-1}\left(\frac{1}{s^{1-\beta}}\right) = h(t) = \frac{1}{t^{\beta}\Gamma(1-\beta)} \tag{32}$$

$$F_{\beta}\left(-H_i, \tau\right) = L^{-1}\left(\frac{1}{p^{\beta}+H_i}\right) = \sum_{n=0}^{\infty}\frac{(-H_i)^n \tau^{(n+1)\beta-1}}{\Gamma\left((n+1)\beta\right)} \tag{33}$$

where $H_i = H_4$ and H_6.

$F_{\beta}(.,.)$ shows Robotnov and Hartleys' function which is given by [51].

After some mathematical calculation Eq. (31) can be written in more suitable form as:

$$\begin{aligned} w_s(n,\tau) &= \left(\frac{G\left(1-(-1)^n\right)+\sigma_n^2+\lambda\sigma_n^4}{\sigma_n\left(\sigma_n^2+\lambda\sigma_n^4\right)}\right) \\ &+\left(\left(\frac{G\left(1-(-1)^n\right)+\sigma_n^2+\lambda\sigma_n^4}{\sigma_n\left(AH_1+\sigma_n^2+\lambda\sigma_n^4\right)}\right)h(t)*F_{\beta}\left(-H_6,\tau\right)\right) \\ &-\left(\left(\frac{G\left(1-(-1)^n\right)+\sigma_n^2+\lambda\sigma_n^4}{\sigma_n\left(\sigma_n^2+\lambda\sigma_n^4\right)}\right)h(t)*F_{\beta}\left(-H_6,\tau\right)\right) \\ &+\left[\begin{array}{l} BH_3H_5-\dfrac{BH_3H_5\left(H_2-H_4\right)^2}{\left(H_4-H_6\right)}1*F_{\beta}\left(-H_4,\tau\right) \\ +\dfrac{BH_3H_5\left(H_2-H_6\right)^2}{\left(H_4-H_6\right)}1*F_{\beta}\left(-H_6,\tau\right)\end{array}\right]. \end{aligned} \tag{34}$$

Equation (34) can be written in more appropriate form as:

$$\begin{aligned} w_s(n,\tau) &= \left(\begin{array}{l} \dfrac{\left(1-(-1)^n\right)}{\sigma_n}+\dfrac{(-1)^n}{\sigma_n} \\ -\dfrac{G\left(1-(-1)^n\right)}{\sigma_n} \\ +\dfrac{G\left(1-(-1)^n\right)}{\sigma_n^3} \\ +\dfrac{G\left(1-(-1)^n\right)}{\left(1+\sigma_n^2\right)}\end{array}\right) \\ &+\left(\alpha_n h(t)*F_{\beta}\left(-H_6,\tau\right)\right) \\ &-\left(\beta_n h(t)*F_{\beta}\left(-H_6,\tau\right)\right) \\ &+\left[\begin{array}{l}\chi_n-\gamma_n\left(1*F_{\beta}\left(-H_4,\tau\right)\right) \\ +\ell_n\left(1*F_{\beta}\left(-H_6,\tau\right)\right)\end{array}\right]. \end{aligned} \tag{35}$$

Now, applying the inverse sine-Fourier transform to Eq. (35), we obtain the following form [52], [53].

$$\begin{aligned} w(\xi,\tau) &= \left(\begin{array}{l} 1-G-\left(\dfrac{1}{h}-\dfrac{Gh}{2}\right)\xi \\ -\dfrac{G}{2}\xi^2+G\left\{\dfrac{\cosh\left(\dfrac{h}{2}-\xi\right)}{\cosh\left(\dfrac{h}{2}\right)}\right\}\end{array}\right) \\ &+\frac{2}{h}\sum_{n=1}^{\infty}\left[\begin{array}{l}\alpha_n h(t)*F_{\beta}\left(-H_6,\tau\right) \\ -\beta_n h(t)*F_{\beta}\left(-H_6,\tau\right)\end{array}\right]\sin\left(\sigma_n\xi\right) \\ &+\frac{2}{h}\sum_{n=1}^{\infty}\left[\begin{array}{l}\chi_n-\gamma_n\left(1*F_{\beta}\left(-H_4,\tau\right)\right) \\ +\ell_n\left(1*F_{\beta}\left(-H_6,\tau\right)\right)\end{array}\right]\sin\left(\sigma_n\xi\right), \end{aligned} \tag{36}$$

where

$$\alpha_n = \left(\frac{G\left(1-(-1)^n\right)+\sigma_n^2+\lambda\sigma_n^4}{\sigma_n\left(AH_1+\sigma_n^2+\lambda\sigma_n^4\right)}\right)$$

$$\beta_n = \left(\frac{G\left(1-(-1)^n\right)+\sigma_n^2+\lambda\sigma_n^4}{\sigma_n\left(\sigma_n^2+\lambda\sigma_n^4\right)}\right)$$

$$\chi_n = BH_3H_5,\ \gamma_n = \frac{BH_3H_5\left(H_2-H_4\right)^2}{\left(H_4-H_6\right)}$$

and

$$\ell_n = \frac{BH_3H_5\left(H_2-H_6\right)^2}{\left(H_4-H_6\right)}.$$

Now the total solution is arranged as a combination of post-transient (steady-state solution) and transient solutions, where the post-transient solution $w_p(\xi)$ is given by:

$$w_p(\xi) = 1-G-\left(\frac{1}{h}-\frac{Gh}{2}\right)\xi - \frac{G}{2}\xi^2+G\left\{\frac{\cosh\left(\frac{h}{2}-\xi\right)}{\cosh\left(\frac{h}{2}\right)}\right\}, \tag{37}$$

and the transient solution $w_{\tau}(\xi,\tau)$ is given as:

$$\begin{aligned} w_{\tau}(\xi,\tau) &= \frac{2}{h}\sum_{n=1}^{\infty}\left[\begin{array}{l}\alpha_n h(t)*F_{\beta}\left(-H_6,\tau\right) \\ -\beta_n h(t)*F_{\beta}\left(-H_6,\tau\right)\end{array}\right]\sin\left(\sigma_n\xi\right) \\ &+\frac{2}{h}\sum_{n=1}^{\infty}\left[\begin{array}{l}\chi_n-\gamma_n\left(1*F_{\beta}\left(-H_4,\tau\right)\right) \\ +\ell_n\left(1*F_{\beta}\left(-H_6,\tau\right)\right)\end{array}\right]\sin\left(\sigma_n\xi\right). \end{aligned} \tag{38}$$

IV. LIMITING CASE: (NEWTONIAN FLUID FLOW WITHOUT BUOYANCY EFFECT)

By putting $(\lambda = 0)$ and $(Gr = 0)$ couple stress fluid model can be reduced to the following form:

$$\rho_{nf}\frac{\partial u(y,t)}{\partial t} = G^* + \mu_{nf}\frac{\partial^2 u(y,t)}{\partial y^2}. \tag{39}$$

The dimensionless form of Eq. (39) can be written as:

$$A\frac{\partial w(\xi,\tau)}{\partial \tau} = G + \frac{\partial^2 w(\xi,\tau)}{\partial \xi^2}. \tag{40}$$

Applying AB fractional definition to Eq. (40) we get the following result:

$${}^{AB}\mathbf{D}_{\tau}^{\beta}Aw(\xi,\tau) = G + \frac{\partial^2 w(\xi,\tau)}{\partial \xi^2}. \tag{41}$$

The Laplace transform is applied to Eq. (41) for closed form solutions, we have the following transform solyution:

$$\frac{p^{\beta}H_1A\overline{w}\left(\xi,p\right)}{\left(p^{\beta}+H_2\right)}=\frac{G}{p}+\frac{d^2\overline{w}\left(\xi,p\right)}{d\xi^2}, \tag{42}$$

Apply sine Fourier transform to Eq. (42), we get the following result:

$$\frac{AH_1p^{\beta}}{p^{\beta}+H_2}\overline{w}_s(n,p)=\frac{G\left(1-(-1)^n\right)}{p\sigma_n}+\frac{\sigma_n}{p}-\sigma_n^2\overline{w}_s(n,p) \tag{43}$$

equivalently,

$$\overline{w}_s(n,p)=\left(\frac{G\left(1-(-1)^n\right)+\sigma_n^2}{p\sigma_n}\right)\times\left[\frac{\left(p^{\beta}+H_2\right)}{\left(AH_1p^{\beta}+\sigma_n^2\left(p^{\beta}+H_2\right)\right)}\right], \tag{44}$$

After some calculation, Eq. (44) can be written in the following form:

$$\overline{w}_s(n,p)=\left(\frac{G\left(1-(-1)^n\right)+\sigma_n^2}{\sigma_n}\right)\times\left(\frac{A_1H_2}{A_2p}+\frac{A_1\left(A_2-H_2\right)}{A_2p^{1-\beta}\left(p^{\beta}+A_2\right)}\right). \tag{45}$$

Upon inversion, Eq. (45), gives:

$$w_s(n,\tau)=\left(\frac{G\left(1-(-1)^n\right)+\sigma_n^2}{\sigma_n}\right)\times\left(\frac{A_1H_2}{A_2}+\frac{A_1\left(A_2-H_2\right)}{A_2}h\left(t\right)*F_{\beta}\left(-A_2,\tau\right)\right), \tag{46}$$

where,

$$A_1=\frac{1}{AH_1+\sigma_n^2},A_2=\frac{\sigma_n^2H_2}{AH_1+\sigma_n^2},H_2=\frac{\beta}{1-\beta}.$$

The inverse sine-Fourier transform is applied to Eq. (46) we get the following form [52], [53].

$$w(\xi,\tau)=\left(\begin{array}{c}1-G-\left(\frac{1}{h}-\frac{Gh}{2}\right)\xi\\-\frac{G}{2}\xi^2+G\left\{\frac{\cosh\left(\frac{h}{2}-\xi\right)}{\cosh\left(\frac{h}{2}\right)}\right\}\end{array}\right)+\frac{2}{h}\sum_{n=1}^{\infty}\left[\frac{A_1\left(A_2-H_2\right)}{A_2}h(t)*F_{\beta}\left(-A_2,\tau\right)\right]\sin\left(\sigma_n\xi\right). \tag{47}$$

The solution obtained in Eq. (47) is for Newtonian viscous fluid in the absence of free convection effect:

Steady state and unsteady solutions are given as under:

$$u_p\left(\xi\right)=1-G-\left(\frac{1}{h}-\frac{Gh}{2}\right)\xi-\frac{G\xi^2}{2}+G\left\{\frac{\cosh\left(\frac{h}{2}-\xi\right)}{\cosh\left(\frac{h}{2}\right)}\right\}, \tag{48}$$

transient solutions is given by

$$u_{\tau}\left(\xi,\tau\right)=+\frac{2}{h}\sum_{n=1}^{\infty}\left[\begin{array}{c}\frac{A_1\left(A_2-H_2\right)}{A_2}h(t)\\*F_{\beta}\left(-A_2,\tau\right)\end{array}\right]\sin\left(\sigma_n\xi\right). \tag{49}$$

V. SPECIAL CASES

In this section, we discuss the following two special cases:

A. COUPLE STRESS NANOFLUID MODEL WITHOUT EXTERNAL PRESSURE GRADIENT

By putting $(G=0)$ the governing equation reduce to the following form:

$${}^{AB}\mathbf{D}_{\tau}^{\beta}Aw(\xi,\tau)=\frac{\partial^2w(\xi,\tau)}{\partial\xi^2}-\lambda\frac{\partial^4w(\xi,\tau)}{\partial\xi^4}+B\theta\left(\xi,\tau\right). \tag{50}$$

In order to find the closed form solutions of the above equation apply both the Laplace and sine Fourier transforms we obtain the following result:

$$\frac{AH_1p^{\beta}}{p^{\beta}+H_2}\overline{w}_s(n,p)=\frac{\sigma_n}{p}-\sigma_n^2\overline{w}_s(n,p)+\lambda\frac{\sigma_n^3}{p}-\lambda\sigma_n^4\overline{w}_s(n,p)+B\overline{\theta}_s\left(n,p\right). \tag{51}$$

Multiply $\frac{p^{\beta}+H_2}{AH_1p^{\beta}}$ both sides, we get:

$$\overline{w}_s(n,p)=\left(\frac{\sigma_n^2+\lambda\sigma_n^4}{p\sigma_n}\right)\times\left[\frac{\left(p^{\beta}+H_2\right)}{\left(AH_1p^{\beta}+\sigma_n^2\left(p^{\beta}+H_2\right)+\lambda\sigma_n^4\left(p^{\beta}+H_2\right)\right)}\right]+B\overline{\theta}_s\left(n,p\right)\times\left[\frac{\left(p^{\beta}+H_2\right)}{\left(AH_1p^{\beta}+\sigma_n^2\left(p^{\beta}+H_2\right)+\lambda\sigma_n^4\left(p^{\beta}+H_2\right)\right)}\right]. \tag{52}$$

After some mathematical calculations the above equation reduced to the following form:

$$\overline{w}_s(n,p)=\left(\frac{\sigma_n^2+\lambda\sigma_n^4}{p\sigma_n}\right)\times\left[\frac{H_5\left(p^{\beta}+H_2\right)}{\left(p^{\beta}+H_6\right)}\right]+B\overline{\theta}_s\left(n,p\right)\times\left[\frac{H_5\left(p^{\beta}+H_2\right)}{\left(p^{\beta}+H_6\right)}\right]. \tag{53}$$

Applying partial fraction, we get the following result:

$$\overline{w}_s(n,p)=\left(\frac{\sigma_n^2+\lambda\sigma_n^4}{\sigma_n}\right)\times\left(\frac{H_5H_2}{H_6p}+\frac{H_5\left(H_6-H_2\right)}{H_6p^{1-\beta}\left(p^{\beta}+H_6\right)}\right)+BH_3H_5\left[\begin{array}{c}\frac{1}{p}-\frac{\left(H_2-H_4\right)^2}{\left(H_4-H_6\right)p\left(p^{\beta}+H_4\right)}\\+\frac{\left(H_2-H_6\right)^2}{\left(H_4-H_6\right)p\left(p^{\beta}+H_6\right)}\end{array}\right]. \tag{54}$$

The inverse Laplace transform gives:

$$w_s(n,\tau) = \left(\frac{\sigma_n^2+\lambda\sigma_n^4}{\sigma_n}\right) \times \left(\frac{H_5H_2}{H_6} + \frac{H_5(H_6-H_2)}{H_6}h(t) * F_\beta(-H_6,\tau)\right) + BH_3H_5\begin{bmatrix} 1 - \frac{(H_2-H_4)^2}{(H_4-H_6)}1 * F_\beta(-H_4,\tau) \\ + \frac{(H_2-H_6)^2}{(H_4-H_6)}1 * F_\beta(-H_6,\tau)\end{bmatrix}, \quad (55)$$

where

$$L^{-1}\left(\frac{1}{s^{1-\beta}}\right) = h(t) = \frac{1}{t^\beta\Gamma(1-\beta)} \quad (56)$$

$$F_\beta(-H_i,\tau) = L^{-1}\left(\frac{1}{p^\beta+H_i}\right) = \sum_{n=0}^{\infty}\frac{(-H_i)^n\tau^{(n+1)\beta-1}}{\Gamma((n+1)\beta)} \quad (57)$$

where $H_i = H_4$ and H_6.

$F_\beta(.,.)$ represents Robotnov and Hartleys' function [51].

Equation (55) can be written in more appropriate form as:

$$w_s(n,\tau) = \left(\frac{\sigma_n^2+\lambda\sigma_n^4}{\sigma_n\left(\sigma_n^2+\lambda\sigma_n^4\right)}\right) + \left(\left(\frac{\sigma_n^2+\lambda\sigma_n^4}{\sigma_n\left(AH_1+\sigma_n^2+\lambda\sigma_n^4\right)}\right)h(t) * F_\beta(-H_6,\tau)\right) - \left(\left(\frac{\sigma_n^2+\lambda\sigma_n^4}{\sigma_n\left(\sigma_n^2+\lambda\sigma_n^4\right)}\right)h(t) * F_\beta(-H_6,\tau)\right) + \begin{bmatrix} BH_3H_5 - \frac{BH_3H_5(H_2-H_4)^2}{(H_4-H_6)}1 * F_\beta(-H_4,\tau) \\ + \frac{BH_3H_5(H_2-H_6)^2}{(H_4-H_6)}1 * F_\beta(-H_6,\tau)\end{bmatrix}. \quad (58)$$

Equation (58) can be written in the more appropriate form as:

$$w_s(n,\tau) = \left(\frac{(1-(-1)^n)}{\sigma_n} + \frac{(-1)^n}{\sigma_n}\right) + \left(\alpha_n h(t) * F_\beta(-H_6,\tau)\right) - \left(\beta_n h(t) * F_\beta(-H_6,\tau)\right) + \begin{bmatrix}\chi_n - \gamma_n\left(1 * F_\beta(-H_4,\tau)\right) \\ + \ell_n\left(1 * F_\beta(-H_6,\tau)\right)\end{bmatrix}. \quad (59)$$

After applying the inverse Fourier transform to Eq. (59) we get the following form [52], [53].

$$w(\xi,\tau) = 1 - \frac{\xi}{h} + \frac{2}{h}\sum_{n=1}^{\infty} \times \begin{bmatrix}\alpha_{n1}h(t) * F_\beta(-H_6,\tau) \\ -\beta_{n1}h(t) * F_\beta(-H_6,\tau)\end{bmatrix}\sin(\sigma_n\xi) + \frac{2}{h}\sum_{n=1}^{\infty}\begin{bmatrix}\chi_n - \gamma_n\left(1 * F_\beta(-H_4,\tau)\right) \\ + \ell_n\left(1 * F_\beta(-H_6,\tau)\right)\end{bmatrix}\sin(\sigma_n\xi), \quad (60)$$

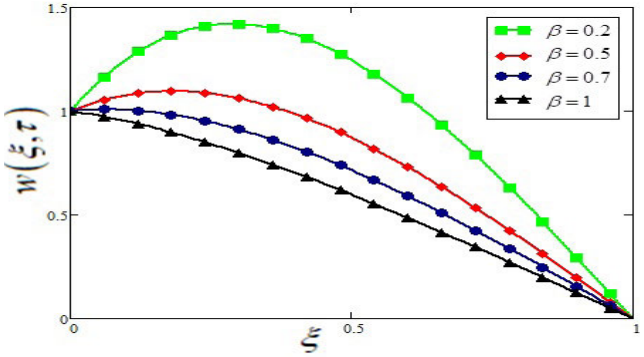

FIGURE 2. Velocity profile of gold in blood CSNF for different values of β when $G = 2$, $\mathrm{Re} = 0.2$, $Gr = 1.5$, $\tau = 0.2$, $\lambda = 0.2$ and $\phi = 0.01$.

where

$$\alpha_{n1} = \left(\frac{\sigma_n^2+\lambda\sigma_n^4}{\sigma_n\left(AH_1+\sigma_n^2+\lambda\sigma_n^4\right)}\right)$$

$$\beta_{n1} = \left(\frac{\sigma_n^2+\lambda\sigma_n^4}{\sigma_n\left(\sigma_n^2+\lambda\sigma_n^4\right)}\right), \chi_n = BH_3H_5,$$

$$\gamma_n = \frac{BH_3H_5(H_2-H_4)^2}{(H_4-H_6)} \text{ and}$$

$$\ell_n = \frac{BH_3H_5(H_2-H_6)^2}{(H_4-H_6)}.$$

B. CLASSICAL MODEL OF REGULAR COUPLE STRESS FLUID

The solutions obtained in Eq.(47) is for a fractional model of Couple Stress nanofluid. The corresponding solutions for classical Couple stress fluid model are obtained by substituting $\beta = 1$ and $\phi = 0$, Eq. (47), as:

$$w(\xi,\tau) = 1 - G - \left(\frac{1}{h} - \frac{Gh}{2}\right)\xi - \frac{G\xi^2}{2} + G\left\{\frac{\cosh\left(\frac{h}{2}-\xi\right)}{\cosh\left(\frac{h}{2}\right)}\right\} - \frac{2}{h}\sum_{n=1}^{\infty}\left(\frac{\frac{G(1-(-1)^n)}{\sigma_n^3(1+\sigma_n^2)}}{+\frac{1}{\sigma_n}}\right)\sin(\sigma_n\xi)\, e^{-\left(\frac{\sigma_n^2+\lambda\sigma_n^4}{\mathrm{Re}}\right)\tau}. \quad (61)$$

The solutions obtained in Eq. (61) is the same as obtained by Akhtar and Shah [Eq. (1), 36], hence this verifies the correctness of the present work.

VI. NUSSELT NUMBER AND SKIN FRICTION

A. NUSSELT NUMBER

The mathematical expression of Nusselt number Nu for CSNF is given as

$$Nu = -\frac{k_{nf}}{k_f}\left(\frac{\partial\theta}{\partial\xi}\right)_{\xi=0}. \quad (62)$$

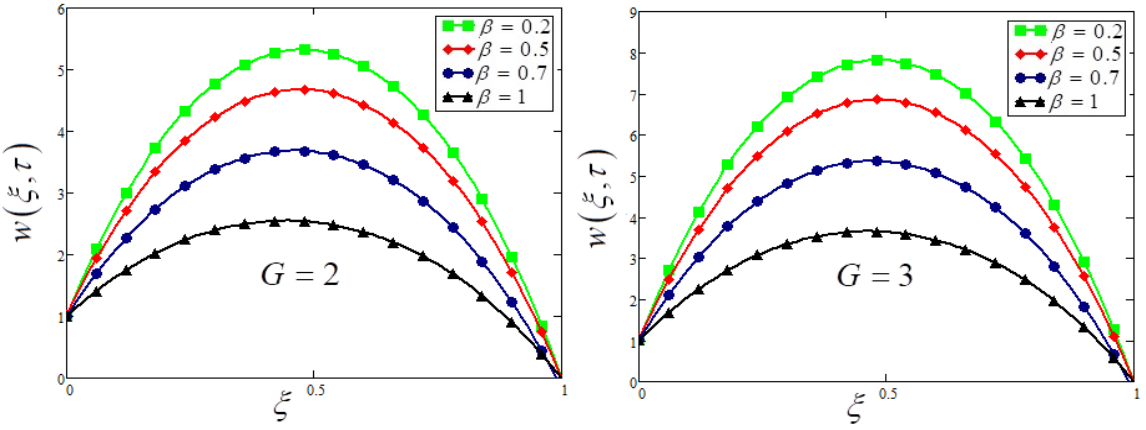

FIGURE 3. Variation in couple stress nanofluid CSNF velocity for different values of pressure gradient G when Re = 0.2, $Gr = 1.5$, $\tau = 0.2$, $\lambda = 0.2$ and $\phi = 0.01$.

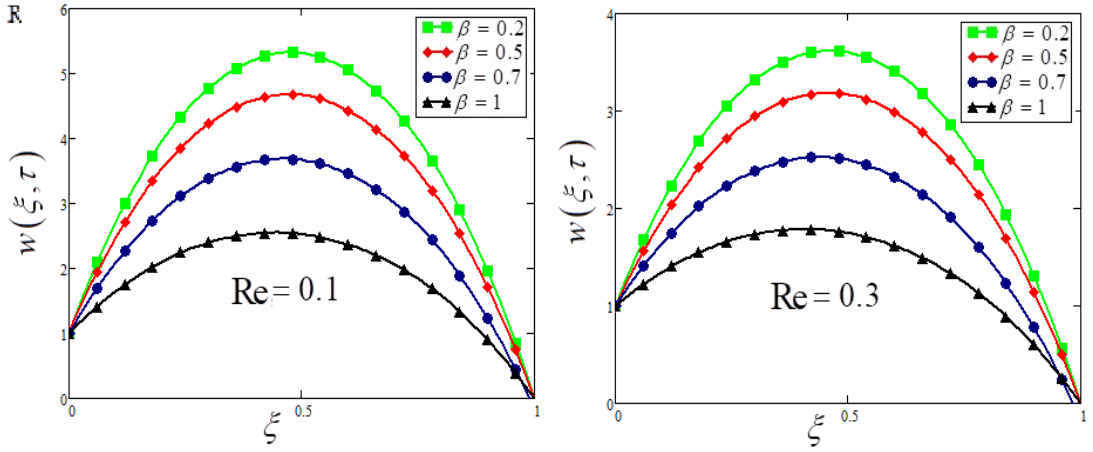

FIGURE 4. Variation in CSNF velocity for different values of Reynolds number Re when $G = 2$, $Gr = 1.5$, $\tau = 0.2$, $\lambda = 0.2$ and $\phi = 0.01$.

B. SKIN FRICTION

The mathematical expression of skin friction for Couple stress nanofluid is given as

$$Sf\,(\xi,\tau) = \frac{1}{(1-\phi)^{2.5}}\left(\frac{\partial w}{\partial \xi} - \frac{\partial^3 w}{\partial \xi^3}\right). \tag{63}$$

As we have CSNF in channel bounded by twow parallel plates. Therefore, the mathematical representation of Skin friction at the lower plate can be written as

$$Sf_{lp}\,(0,\tau) = \frac{1}{(1-\phi)^{2.5}}\left(\frac{\partial w}{\partial \xi} - \frac{\partial^3 w}{\partial \xi^3}\right). \tag{64}$$

where $Cf_{lp}(,)$ shows skin friction at the lower plate. Similarly, the mathematical expression of skin friction at the upper plate is given as:

$$Sf_{up}\,(1,\tau) = \frac{1}{(1-\phi)^{2.5}}\left(\frac{\partial w}{\partial \xi} - \frac{\partial^3 w}{\partial \xi^3}\right). \tag{65}$$

where $Cf_{up}(,)$ shows skin friction at the upper plate.

VII. RESULTS AND DISCUSSION

This section of our study consists the results computed numerically in various graphs. Figure 1 shows the geometry of the proposed problem. The obtained results are shown in Figure 2 to 16 for different parameters and for clear understanding. These graphs show the effect of CSNF parameters in a channel.

Variation of the fractional parameter β is shown in the Figure 2. It is found that increasing β results a decrease in CSNF velocity.

It is important to note that in all these graphs the results of Couple stress fluid of fractional order $(0 < \beta < 1)$ and integer order $(\beta = 1)$ are compared in order to clearly see the differences. All these graphs show the flow behavour of CSNF that the classical velocity have lower magnitude as compared to the magnitude of fractional velocity. However, by increasing β there is a decrease in the magnitude of CSNF velocity. For the case, $\beta = 1$ present solution reduced to the solutions obtained by Akhtar [36] which shows the validity of our obtained solutions and verifies the correctness of

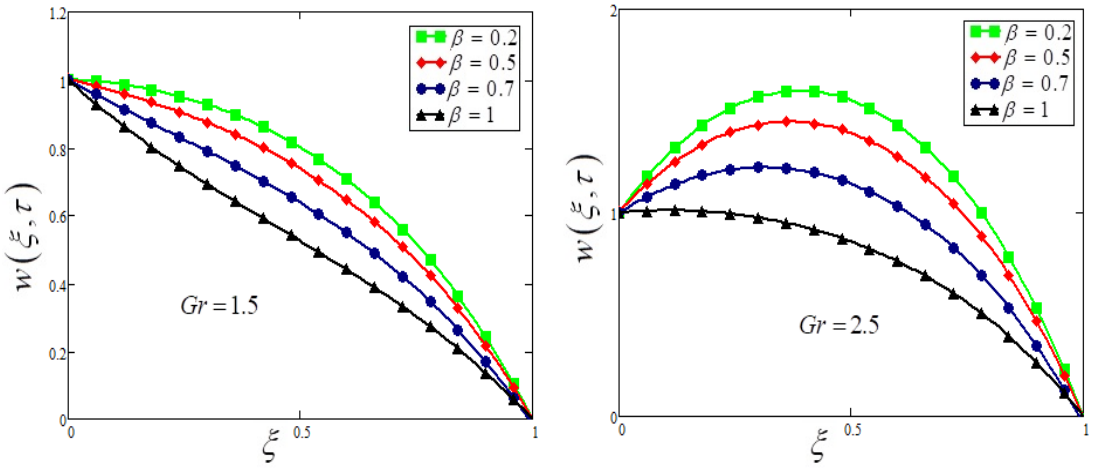

FIGURE 5. Variation in CSNF velocity for different values of Grashof number Gr when $G = 2$, Re $= 0.3$, $\tau = 0.2$, $\lambda = 0.2$ and $\phi = 0.01$.

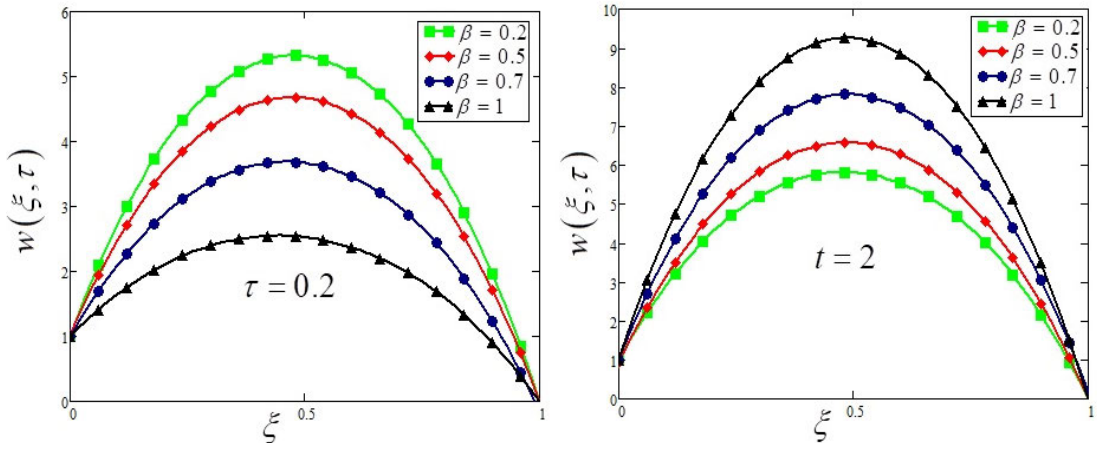

FIGURE 6. Variation in CSNF velocity profile for different values of time τ when $G = 2$, Re $= 0.3$, $Gr = 1.5$, $\lambda = 0.2$ and $\phi = 0.01$.

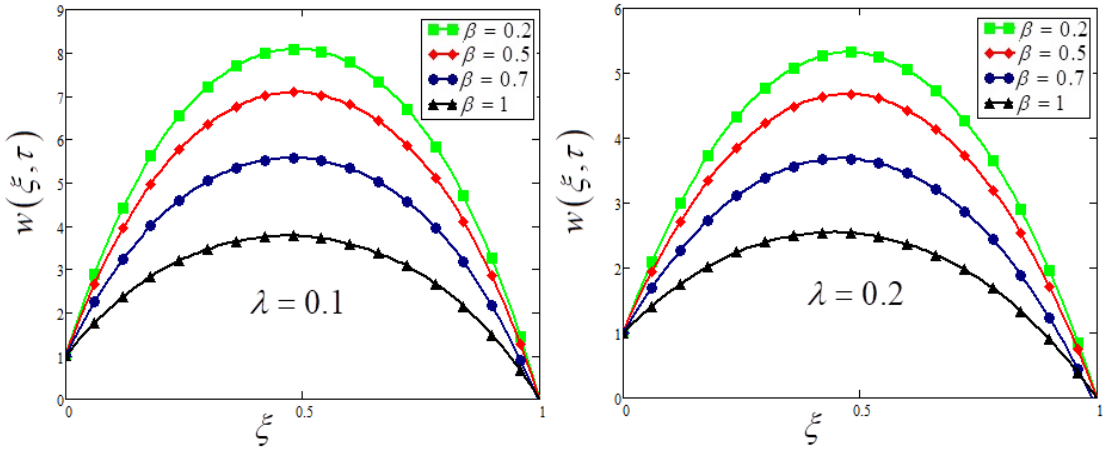

FIGURE 7. Variation in CSNF velocity profile for different values of couple stress parameter λ when $G = 2$, Re $= 0.3$, $Gr = 1.5$, $\tau = 0.2$, $\lambda = 0.2$ and $\phi = 0.01$.

obtained results. Figure 3 depicts the variation in CSNF velocity for different values of external pressure gradient G fluid is moving in a channel. From this figure, it can be noticed that couple stress nanofluid CSNF velocity increases by increasing the absolute value of external pressure gradient G from $G = 2$ to $G = 3$. It is due to the fact that

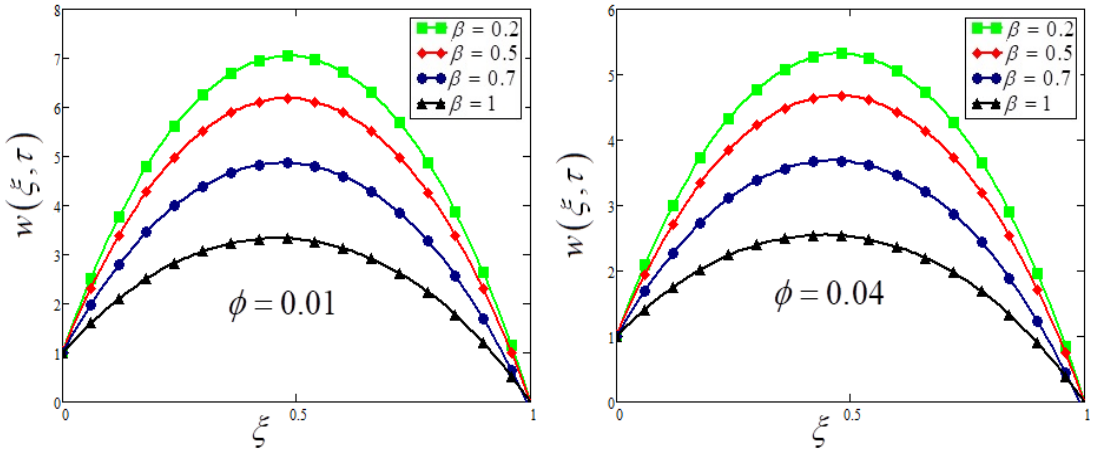

FIGURE 8. Variation in CSNF velocity profile for different values of volume fraction parameter ϕ when $G = 2$, Re $= 0.3$, $Gr = 1.5$, $\tau = 0.2$ and $\lambda = 0.2$.

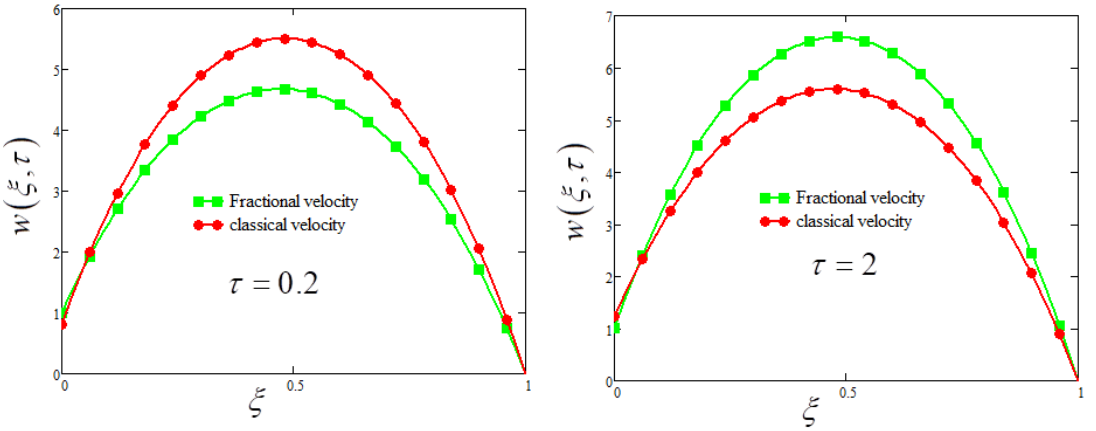

FIGURE 9. Comparison of AB fractional velocity $(0 < \beta < 1)$ with classical velocity when $G = 2$, Re $= 0.3$, $Gr = 1.5$, $\lambda = 0.2$ and $\phi = 0.04$.

increasing external pressure, CSNF becomes thinner due to which viscosity of the fluid decreases, as a result, CSNF velocity accelerates and the magnitude of velocity increases. In other words increasing external pressure gradient speed up the motion of the CSNF in a channel. Furthermore, increasing external pressure will increase the volume flow rate in a channel.

Figure 4 shows the variation of the Reynolds number (Re) on the CSNF fluid velocity. By increasing Re, velocity of the fluids decreases, as Re is the ratio of inertial forces to the viscous forces. By increasing Re of CSNF, it produces turbulent behavior in the fluid flow, due to these turbulent forces CSNF becomes more viscous as a result it controls the flow of the CSNF velocity. From the comparison of the two graphs Re $= 0.1$ and Re $= 0.3$ clearly shows that increasing Reynolds number Re, force the velocity to decreases.

Figure 5 shows the velocity profile of the couple stress nanofluid for different values of Gr. Increasing the value of $Gr = 1.5$ to $Gr = 2.5$, variation in CSNF can be observed. This variation of Gr is obvious in many situations that increase Gr results in an increase in the CSNF velocity. It is due to the fact that Gr shows buoyancy forces when these forces increase the fluid viscosity decreases due to which velocity increases. This effect of Gr is very important and have useful applications in the fluid dynamics.

Figure 6 displays the velocity of couple stress nanofluid CSNF for different values of τ. From this figure, it is clearly seen that for short interval of time $\tau = 0.2$, the magnitude of the CSNF velocity is lower, while for a long time $\tau = 2$, the fluid velocity increases it is due to the fact that we have considered unsteady couple stress nanofluid CSNF in our assumptions. It is further noticed from this figure that for $\tau = 0.2$, the behavior of CSNF velocity decreases with the increase of AB fractional parameter β and for $\tau = 2$, this effect of β reverses on CSNF velocity.

Figure 7 shows the effect of CSNF velocity profile for different values of couple stress parameter λ keeping other values constant. As we have considered gold nanoparticles suspended in blood as base fluid. Usually, when we mix any additives in the fluid the forces (present in the fluid) oppose

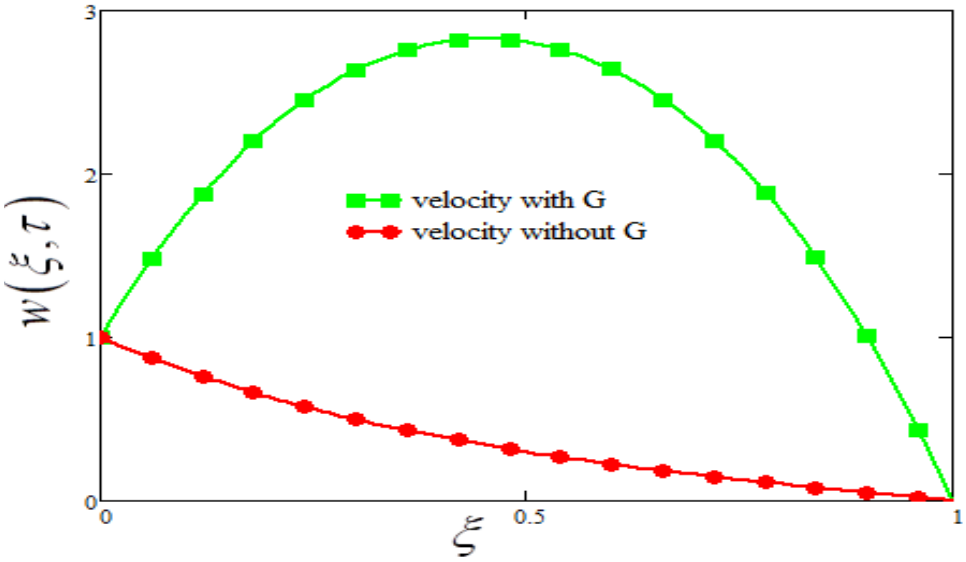

FIGURE 10. Comparison of fractional velocities in the absence ($G = 0$) and presence ($G \neq 0, > 0$) of external pressure when Re $= 0.3$, $Gr = 1.5$, $\tau = 0.2$, $\lambda = 0.2$, $\beta = 0.2$ and $\phi = 0.04$.

the forces generated by additives. This opposite force makes a couple force and a couple stress is induced in the fluid motion. Therefore, Figure 7 clearly show that increasing couple stress parameter $\lambda = 0.1$ to $\lambda = 0.2$, as a result CSNF velocity decreases due to these opposite forces flow of CSNF in the channel decreases.

Figure 8 shows the influence of volume friction parameter ϕ on CSNF velocity. It is found that increasing ϕ from 0.01 to 0.02 CSNF velocity decreases because the density of CSNF velocity increases and finally, the flow of CSNF in a channel resists and as a result the magnitude of velocity slows down.

A comparison of couple stress fluid velocities for fractional and classical orders is made in Figure 9. This figure shows that for smaller time $\tau = 0.2$, classical velocity is maximum while for higher values of time $\tau = 2$, the magnitude of velocity for AB fractional derivative is maximum. This shows that CSNF flow in a channel is affected by fractional parameter β for small and higher values of time the variation is quite the opposite. Furthermore, CSNF is in the class of non-Newtonian fluid and β have dual effect on on-Newtonian fluid for small and large time.

Figure 10 displays a comparison of CSNF flow in the presence and absence of external pressure gradient G. From this figure it is clearly noted that the role of the external pressure gradient G in CSNF velocity is to accelerate the fluid motion and hence fluid achieved maximum velocity.

Figure 11 shows a comparison of CSNF velocity and Newtonian viscous fluid velocity. From this figure, it is clear that the magnitude of velocity for Newtonian viscous fluid is higher than that of couple stress fluid velocity. The nature of Newtonian visvcous fluid and CSNF is quite chage that's why the velocity of these fluids show variations.

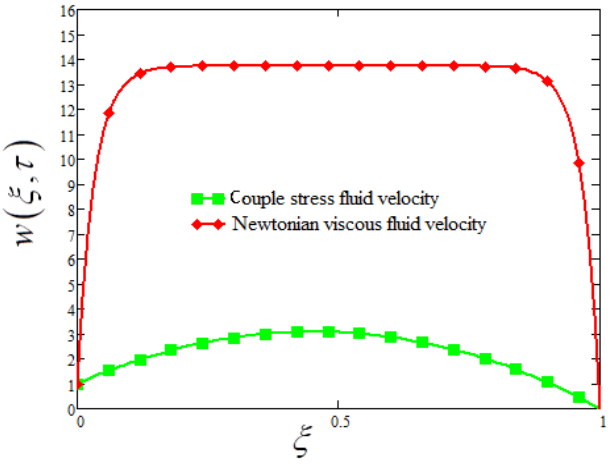

FIGURE 11. Comparison of CSNF velocity with Newtonian viscous fluid velocity when $G = 2$, Re $= 0.2$, $Gr = 1.5$, $\tau = 0.2$, $\beta = 0.2$ and $\phi = 0.01$.

Figure 12 depicts the temperature profile for different values of the time τ. From this figure, it can be seen that the energy profile decreases with the increase of fractional parameter β. This behavior of β on temperature profile is decreasing for time $\tau = 0.2$ and for time $\tau = 2$, this behavior of β is reverses as shown in this figure. The increase in β shows a decrease in temeprature for small time while for large time this behavoiur is opposite.

Figure 13 shows the influence of volume friction parameter ϕ on the temperature profile. More exactly, the graph shows that increasing ϕ results in an increase in the temperature of the CSNF. This behavior of ϕ is studied for two different times i.e. $\tau = 0.2$ and for $\tau = 2$. Furthermore, from this figure, it is observed that the temperature of CSNF velocity

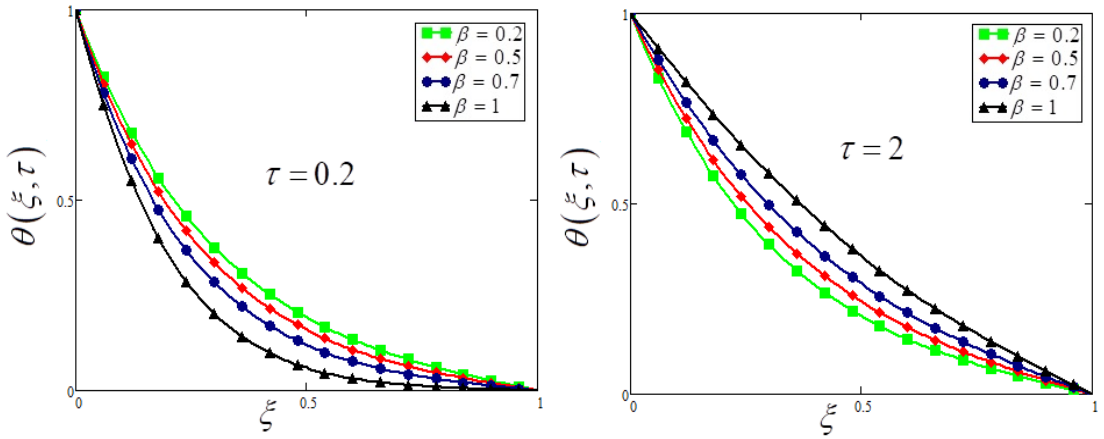

FIGURE 12. Temperature profile for different values of τ (fractional and classical cases). $Pr = 12$, $\beta = 0.2$ and $\phi = 0.01$.

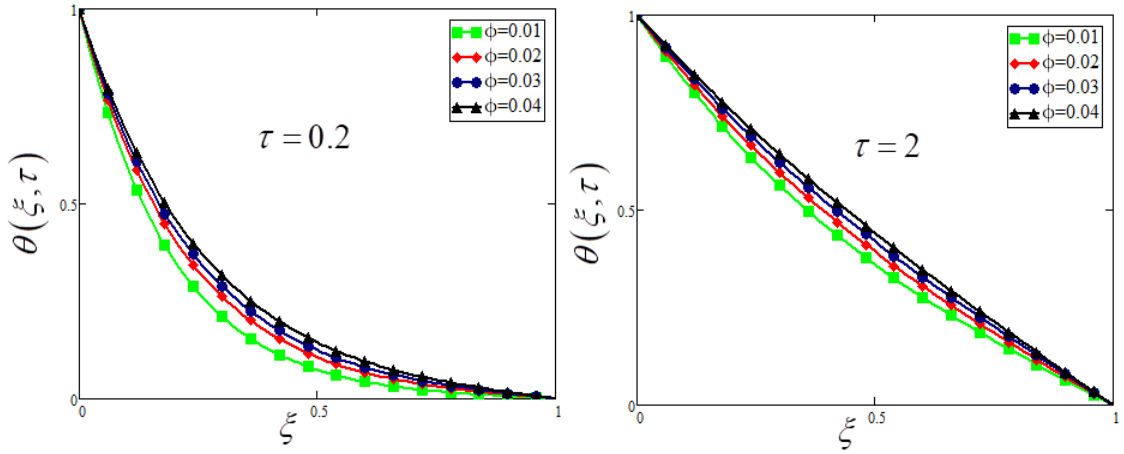

FIGURE 13. Influence of nanoparticles volume fraction on temperature for different times when $\beta = 0.2$ and Pr = 12.

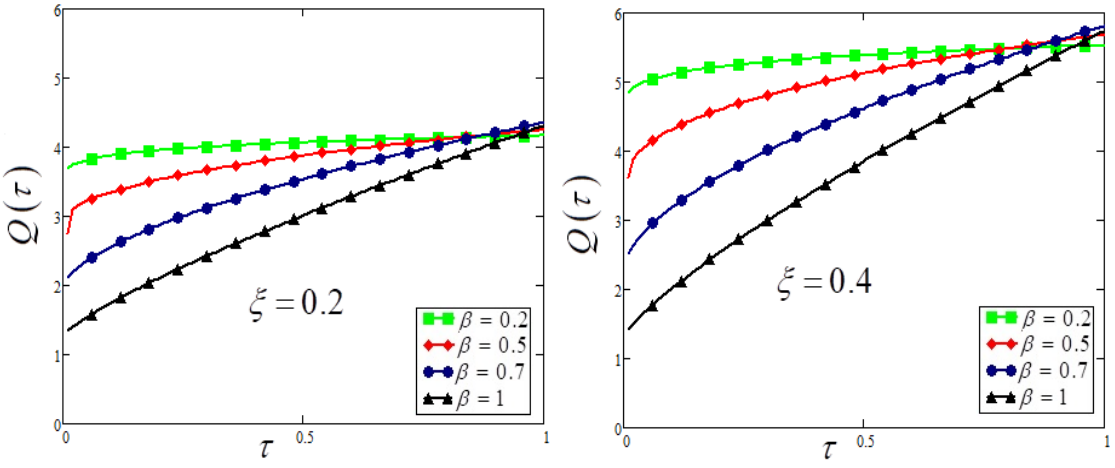

FIGURE 14. Plots of Volume flow rate, along τ, for two different ξ (fractional and classical velocities) when Re = 0.1, $Gr = 1.5$, $\lambda = 0.2$ and $\phi = 0.04$.

increases with time. Furthermore, increasing the valume friction ϕ as a result there will be a maximum collision and as a result the kinetic energy of CSNF is increases.

Figure 14 shows the volume flow rate $Q(\tau)$, along τ for two different ξ. This figure shows that increasing ξ means to increase the distance between the plates which shows

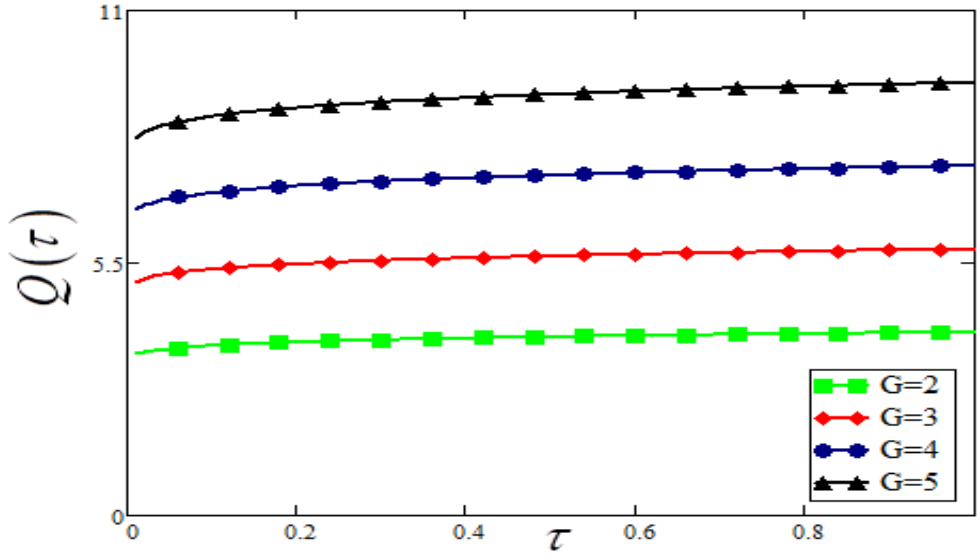

FIGURE 15. Plots of Volume flow rate, along τ, for different G (fractional case $0 < \beta < 1$) when $\mathrm{Re} = 0.1$, $Gr = 1.5$, $\beta = 0.2$, $\lambda = 0.2$ and $\phi = 0.04$.

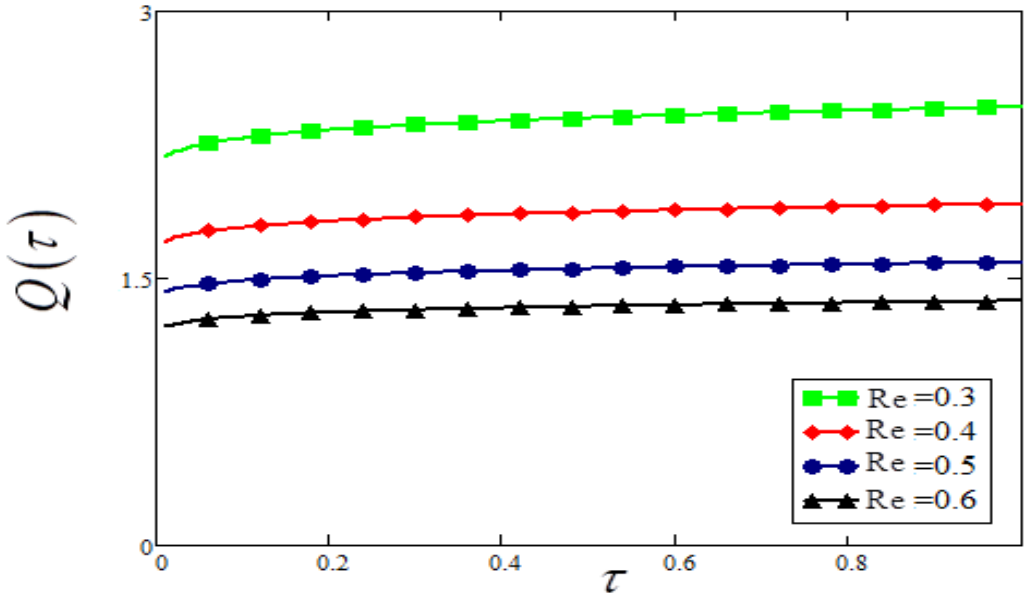

FIGURE 16. Plots of Volume flow rate, along τ, for different Re (fractional case $0 < \beta < 1$) when $Gr = 1.5$, $\beta = 0.2$, $\lambda = 0.2$ and $\phi = 0.04$.

that more and more fluid is passing through the channel. The increase in the distance between the plates is directly proportional to the volume flow rate. Figure 15 depicts the volume flow rate $Q(\tau)$ along τ, of CSNF flow in a channel with the variation in G. By increasing G the rate of volume flow is increases because G accelerate the flow due to which the more volume of the CSNF passes through the channel. Furthermore, the increase in external pressure gradient G will increase the volume flow rate at the centre of the channel. Figure 16 shows the volume flow rate $Q(\tau)$, along τ for different Reynolds number Re, (fractional case, $0 < \beta < 1$) on the CSNF velocity in a channel. From this figure, we observed that the rate of volume flow-through the channel is affected by Re, because Re, controls the fluid motion due to which less fluid will pass through the channel. Finally, the Nusselt number Nu and skin friction C_f of CSNF at the lower and upper plate are evaluated and presented in tabular forms which are given in Tables 2, 3 and Table 4 respectively. Note that in these the bold numbers show the variation in that specific parameter.

Table 2 and Table 3 show the skin friction variation at lower and upper plate respectively. These tables show the result of

TABLE 2. Skin friction of CSNF at lower plate:(Comparison of fractional and classical results).

G	Re	Gr	τ	λ	ϕ	β	Cf_{β}	$Cf_{classic}$
5	11	1.5	2	0.2	0.02	0.3	9.763	6.391
6	11	1.5	2	0.2	0.02	0.3	12.161	8.037
5	**12**	1.5	2	0.2	0.02	0.3	7.756	4.354
5	11	**2**	2	0.2	0.02	0.3	7.756	8.354
5	11	1.5	**2.5**	0.2	0.02	0.3	10.122	5.816
5	11	1.5	2	**0.3**	0.02	0.3	7.571	3.795
5	11	1.5	2	0.2	**0.04**	0.3	7.867	4.263
5	11	1.5	2	0.2	0.02	**0.5**	13.161	6.391

TABLE 3. Skin friction of CSNF at upper plate:(Comparison of fractional and classical results).

G	Re	Gr	τ	λ	ϕ	β	Cf_{β}	$Cf_{classic}$
5	0.6	1.3	2	0.2	0.02	0.3	12.555	11.266
6	0.6	1.3	2	0.2	0.02	0.3	14.953	13.41
5	**0.7**	1.3	2	0.2	0.02	0.3	10.523	9.42
5	0.6	**2**	2	0.2	0.02	0.3	15.321	14.953
5	0.6	1.3	**2.5**	0.2	0.02	0.3	12.919	11.321
5	0.6	1.3	2	**0.3**	0.02	0.3	10.201	9.176
5	0.6	1.3	2	0.2	**0.04**	0.3	10.776	9.639
5	0.6	1.3	2	0.2	0.02	**0.5**	16.137	11.341

TABLE 4. Nusselt number for couple stress Nanofluid.

β	ϕ	τ	Nu
0.2	0.02	0.5	0.293
0.3	0.02	0.5	0.288
0.2	**0.03**	0.5	0.312
0.2	0.02	**0.6**	0.295

skin friction variation for fractional and classical model of CSNF. In the tables the bold values show the Skin friction variation for G, Re, Gr, τ, λ, β and ϕ.

Table 4 shows the Nusselt number variation for couple stress nanofluid. The bolds values in the table shows the Nusselt number for β, τ and ϕ.

VIII. CONCLUDING REMARKS

The aim of this study is to obtain an exact solution for the couple stress nanofluid CSNF in a channel. The solutions obtained for AB fractional derivative are shown in graphs. Blood is considered as base fluid and gold (Au) is taken as nanoparticles. The obtained solutions satisfy the initial and boundary conditions. Some special cases are deduced and published results in the literature are recovered for accuracy purpose. Furthermore, AB fractional derivatives are applied to the couple stress nanofluid CSNF model to compare their effect on velocity profile for small and large times.

The key points are listed below.

- The effect of AB fractional derivatives is shown in the velocity profile. From the graphical results, we noticed that for a short time the magnitude of CSNF velocity decreases with an increase in β while for $\tau = 2$ the magnitude of velocity increases with the increase in β.
- Increasing external pressure gradient CSNF velocity increases.
- The velocity of the CSNF decreases by increasing the values of Re.
- Increasing time t, velocity of the CSNF increase.
- Increasing the volume fraction ϕ velocity of CSNF decreases.
- The velocity of Newtonian viscous fluid is higher than CSNF velocity.
- By increasing Gr, CSNF velocity increases.
- By increases ϕ temperature of CSNF increases.
- Volume flow rate increases with G and ξ while decreases with Re.

REFERENCES

[1] V. K. Stokes, "Couple stresses in fluids," *Phys. Fluids*, vol. 9, no. 9, pp. 1709–1715, 1966.
[2] S. Vk, *Theories of Fluids With Microstructure*. New York, NY, USA: Springer; 1984.
[3] N. B. Naduvinamani, P. S. Hiremath, and G. Gurubasavaraj, "Squeeze film lubrication of a short porous journal bearing with couple stress fluids," *Tribol. Int.*, vol. 34, no. 11, pp. 739–747, Nov. 2001.

[4] B. Mahanthesh, B. J. Gireesha, M. Sheikholeslami, S. A. Shehzad, and P. B. S. Kumar, "Nonlinear radiative flow of casson nanoliquid past a cone and wedge with magnetic dipole: Mathematical model of renewable energy," *J. Nanofluids*, vol. 7, no. 6, pp. 1089–1100, Dec. 2018.
[5] B. Mahanthesh, B. J. Gireesha, N. S. Shashikumar, T. Hayat, and A. Alsaedi, "Marangoni convection in casson liquid flow due to an infinite disk with exponential space dependent heat source and cross-diffusion effects," *Results Phys.*, vol. 9, pp. 78–85, Jun. 2018.
[6] G. Ramanaiah, "Squeeze films between finite plates lubricated by fluids with couple stress," *Wear*, vol. 54, no. 2, pp. 315–320, Jun. 1979.
[7] P. Sinha and C. Singh, "Couple stresses in the lubrication of rolling contact bearings considering cavitation," *Wear*, vol. 67, no. 1, pp. 85–98, Mar. 1981.
[8] J.-R. Lin, "Squeeze film characteristics between a sphere and a flat plate: Couple stress fluid model," *Comput. Struct.*, vol. 75, no. 1, pp. 73–80, Mar. 2000.
[9] A. Banyal, "The necessary condition for the onset of stationary convection in couple-stress fluid," *Int. J. Fluid Mech. Res.*, vol. 38, no. 5, pp. 450–457, 2011.
[10] M. Devakar, D. Sreenivasu, and B. Shankar, "Analytical solutions of some fully developed flows of couple stress fluid between concentric cylinders with slip boundary conditions," *Int. J. Eng. Math.*, vol. 2014, May 2014, Art. no. 785396.
[11] M. Devakar and T. K. V. Iyengar, "Run up flow of a couple stress fluid between parallel plates," *Nonlinear Anal., Model. Control*, vol. 15, no. 1, pp. 29–37, 2010.
[12] A. A. Opanuga, H. I. O. O. Okagbue Agboola, and S. A. Bishop, "Second law analysis of ion slip effect on MHD couple stress fluid," *Int. J. Mech.*, vol. 12, pp. 96–101, May 2018.
[13] N. A. Khan, H. Khan, and S. A. Ali, "Exact solutions for MHD flow of couple stress fluid with heat transfer," *J. Egyptian Math. Soc.*, vol. 24, no. 1, pp. 125–129, Jan. 2016.
[14] T. Hayat, M. Awais, A. Safdar, and A. A. Hendi "Unsteady three dimensional flow of couple stress fluid over a stretched surface with chemical reaction," *Nonlinear Anal, Modell Control*, vol. 17, no. 1, pp. 47–59.
[15] K. Naeem, "A class of flows for couple stress fluids," *J. Basic Appl. Sci.*, pp. 97–104, Jan. 2012.
[16] O. A. Bég, S. K. Ghosh, S. Ahmed, and T. Bég, "Mathematical modeling of oscillatory magneto-convection of a couple-stress biofluid in an inclined rotating channel," *J. Mech. Med. Biol.*, vol. 12, no. 3, Jun. 2012, Art. no. 1250050.
[17] S. O. Adesanya and O. D. Makinde, "Effects of couple stresses on entropy generation rate in a porous channel with convective heating," *Comput. Appl. Math.*, vol. 34, no. 1, pp. 293–307, Apr. 2015.
[18] S. O. Adesanya and O. D. Makinde, "Irreversibility analysis in a couple stress film flow along an inclined heated plate with adiabatic free surface," *Phys. A, Stat. Mech. Appl.*, vol. 432, pp. 222–229, Aug. 2015.
[19] N. B. Naduvinamani, S. Tasneem Fathima, and P. S. Hiremath, "Effect of surface roughness on characteristics of couplestress squeeze film between anisotropic porous rectangular plates," *Fluid Dyn. Res.*, vol. 32, no. 5, pp. 217–231, May 2003.
[20] J.-R. Lin and C.-R. Hung, "Combined effects of non-newtonian couple stresses and fluid inertia on the squeeze film characteristics between a long cylinder and an infinite plate," *Fluid Dyn. Res.*, vol. 39, no. 8, pp. 616–631, Aug. 2007.
[21] R.-F. Lu and J.-R. Lin, "A theoretical study of combined effects of non-newtonian rheology and viscosity-pressure dependence in the sphere-plate squeeze-film system," *Tribol. Int.*, vol. 40, no. 1, pp. 125–131, Jan. 2007.
[22] E. A. Ashmawy, "Unsteady couette flow of a micropolar fluid with slip," *Meccanica*, vol. 47, no. 1, pp. 85–94, Jan. 2012.
[23] K. Oldham and J. Spanier, *The Fractional Calculus Theory and Applications of Differentiation and Integration to Arbitrary Order*, vol. 111. Amsterdam, The Netherlands: Elsevier, 1974.
[24] D. A. Benson, "The fractional advection-dispersion equation: Development and application," Ph.D. dissertation, Dept. Hydrogeol., Univ. Nevada, Reno, NV, USA, 1998.
[25] W. E. Olmstead and R. A. Handelsman, "Diffusion in a semi-infinite region with nonlinear surface dissipation," *SIAM Rev.*, vol. 18, no. 2, pp. 275–291, Apr. 1976.
[26] R. Marks and M. Hall, "Differintegral interpolation from a bandlimited signal's samples," *IEEE Trans. Acoust., Speech, Signal Process.*, vol. 29, no. 4, pp. 872–877, Aug. 1981.
[27] E. Cuesta, M. Kirane, and S. A. Malik. *Anisotropic Like Approach to Image Denoising by Means of Generalized Fractional Time Integrals*. [Online]. Available: http://hal.archives-ouvertes.fr/hal-00437341/fr
[28] A. Freed, K. Diethelm, and Y. Luchko, "Fractional-order viscoelasticity (FOV): Constitutive development using the fractional calculus: First annual report," NASA Glenn Res. Center, Cleveland, OH, USA, Tech. Rep. NASA/TM-2002-211914, NAS 1.15:211914, E-13607, 2002.
[29] L. Gaul, P. Klein, and S. Kemple, "Damping description involving fractional operators," *Mech. Syst. Signal Process.*, vol. 5, no. 2, pp. 81–88, Mar. 1991.
[30] I. Podlubny, "Application of fractional-order derivatives to calculation of heat load intensity change in blast furnace walls," *Transl.-Ve Riecansky*, no. 2, pp. 137–144, 1995.
[31] B. J. West, "Fractional calculus in bioengineering," *J. Stat. Phys.*, vol. 126, no. 6, pp. 1285–1286, Apr. 2007.
[32] M. Caputo and M. Fabrizio, "A new definition of fractional derivative without singular kernel," *Prog. Fractional Differ. Appl.*, vol. 1, no. 2, pp. 1–13, 2015.
[33] A. Atangana and J. J. Nieto, "Numerical solution for the model of RLC circuit via the fractional derivative without singular kernel," *Adv. Mech. Eng.*, vol. 7, no. 10, Oct. 2015, Art. no. 168781401561375.
[34] A. Atangana, "On the new fractional derivative and application to nonlinear Fisher's reaction–diffusion equation," *Appl. Math. Comput.*, vol. 273, pp. 948–956, Jan. 2016.
[35] M. Arif, F. Ali, N. A. Sheikh, I. Khan, and K. S. Nisar, "Fractional model of couple stress fluid for generalized couette flow: A comparative analysis of Atangana–Baleanu and Caputo–Fabrizio fractional derivatives," *IEEE Access*, vol. 7, pp. 88643–88655, 2019.
[36] S. Akhtar, "Flows between two parallel plates of couple stress fluids with time-fractional caputo and caputo-fabrizio derivatives," *Eur. Phys. J. Plus*, vol. 131, no. 11, Nov. 2016.
[37] S. U. Choi and J. A. Eastman, "Enhancing thermal conductivity of fluids with nanoparticles," Argonne Nat. Lab., Lemont, IL, USA, Tech. Rep. ANL/MSD/CP-84938 CONF-951135-29, 1995.
[38] M. Ramzan, "Influence of newtonian heating on three dimensional MHD flow of couple stress nanofluid with viscous dissipation and joule heating," *PLoS ONE*, vol. 10, no. 4, 2015, Art. no. e0124699.
[39] T. Hayat, A. Aziz, T. Muhammad, and B. Ahmad, "Influence of magnetic field in three-dimensional flow of couple stress nanofluid over a nonlinearly stretching surface with convective condition," *PLoS ONE*, vol. 10, no. 12, 2015, Art. no. e0145332.
[40] M. Arif, F. Ali, N. A. Sheikh, and I. Khan, "Enhanced heat transfer in working fluids using nanoparticles with ramped wall temperature: Applications in engine oil," *Adv. Mech. Eng.*, vol. 11, no. 11, Nov. 2019, Art. no. 168781401988098.
[41] M. Awais, S. Saleem, T. Hayat, and S. Irum, "Hydromagnetic couple-stress nanofluid flow over a moving convective wall: OHAM analysis," *Acta Astronautica*, vol. 129, pp. 271–276, Dec. 2016.
[42] B. J. Gireesha, B. Mahanthesh, and M. M. Rashidi, "MHD boundary layer heat and mass transfer of a chemically reacting Casson fluid over a permeable stretching surface with non-uniform heat source/sink," *Int. J. Ind. Math.*, vol. 7, no. 3, pp. 247–260, 2015.
[43] B. J. Gireesha, P. B. S. Kumar, B. Mahanthesh, S. A. Shehzad, and A. Rauf, "Nonlinear 3D flow of casson-carreau fluids with homogeneous–heterogeneous reactions: A comparative study," *Results Phys.*, vol. 7, pp. 2762–2770, May 2017.
[44] B. Mahanthesh and B. J. Gireesha, "Scrutinization of thermal radiation, viscous dissipation and joule heating effects on marangoni convective two-phase flow of casson fluid with fluid-particle suspension," *Results Phys.*, vol. 8, pp. 869–878, Mar. 2018.
[45] K. Ramesh, "Influence of heat and mass transfer on peristaltic flow of a couple stress fluid through porous medium in the presence of inclined magnetic field in an inclined asymmetric channel," *J. Mol. Liquids*, vol. 219, pp. 256–271, Jul. 2016.
[46] K. G. Binu, B. S. Shenoy, D. S. Rao, and R. Pai, "Static characteristics of a fluid film bearing with TiO2 based nanolubricant using the modified Krieger–Dougherty viscosity model and couple stress model," *Tribology Int.*, vol. 75, pp. 69–79, Jul. 2014.
[47] B. J. Gireesha, M. Archana, B. Mahanthesh, and B. C. Prasannakumara, "Exploration of activation energy and binary chemical reaction effects on nano casson fluid flow with thermal and exponential space-based heat source," *Multidiscipline Model. Mater. Struct.*, vol. 15, no. 1, pp. 227–245, Jan. 2019.

[48] S. Aman, I. Khan, Z. Ismail, and M. Z. Salleh, "Impacts of gold nanoparticles on MHD mixed convection poiseuille flow of nanofluid passing through a porous medium in the presence of thermal radiation, thermal diffusion and chemical reaction," *Neural Comput. Appl.*, vol. 30, no. 3, pp. 789–797, Aug. 2018.
[49] M. Hatami, J. Hatami, and D. D. Ganji, "Computer simulation of MHD blood conveying gold nanoparticles as a third grade non-newtonian nanofluid in a hollow porous vessel," *Comput. Methods Programs Biomed.*, vol. 113, no. 2, pp. 632–641, Feb. 2014.
[50] A. A. Kilbas, M. Saigo, and R. K. Saxena, "Generalized mittag-leffler function and generalized fractional calculus operators," *Integral Transforms Special Functions*, vol. 15, no. 1, pp. 31–49, Feb. 2004.
[51] C. F. Lorenzo and T. T. Hartley, "Generalized functions for the fractional calculus," NASA Glenn Res. Center; Cleveland, OH, USA, Tech. Rep. NASA/TP-1999-209424, NAS 1.60:209424, E-11944, 1999.
[52] L. Debnath and D. Bhatta, *Integral Transforms and Their Applications*, 2nd ed. Boca Raton, FL, USA: CRC Press 2006.
[53] I. S. Gradshteyn and I. M. Ryzhik, *Table of Integrals, Series, and Products*, 7th ed. Amsterdam, The Netherlands: Elsevier, 2007.

MUHAMMAD ARIF received the M.S. degree in applied mathematics from the City University of Science and Information Technology, Peshawar, under the supervision of an Associate Professor Dr. Farhad Ali (HoD Mathematics, CUSIT), and the M.Sc. degree in mathematics from the City University of Science and Information Technology. He has published three research articles in different well-reputed high-impact factor international journals of the world. He has more than eight years of academic experience in different reputed institutions of the city. His most experience has been working in the academic sector and has expertise in the areas of fluid dynamics, two phase flows, MHD flows, nanofluids, couple stress fluid, fractional derivatives, integral transforms, exact solutions, numerical solutions, and mathematical modeling.

FARHAD ALI received the Ph.D. degree in applied mathematics from the Universiti Teknologi Malaysia, one of the world leading Universities. He has over 13 years of academic experience in different reputed institutions of the country. He is currently working as the Dean of sciences and IT with the City University of Science and Information Technology. He is also working as the Head of the Department of Mathematics. He is also the Head of the Computational Analysis Research Group, Ton Duc Thang University, Vietnam. Additionally, he has the charge of Director ORIC. He has published more than 80 research articles in different well-reputed international journals of the world. Apart from academic, he has organized academic knowledge seminars and international conferences for students, faculty members, researchers, and practitioners from different parts of the world. His expertise is in the areas of fluid dynamics, MHD flows, nanofluids, fractional derivatives, integral transforms, exact solutions, and mathematical modeling. He is also an editor of some high ranked journals. He is also a potential reviewer of many research journals of the world. He is the Chief Editor of the *City University International Journal of Computational Analysis*. He is an HEC Approved Supervisor and has supervised dozens of M.S. scholars.

ILYAS KHAN received the Ph.D. degree in applied mathematics from the Universiti Teknologi Malaysia, one of the world leading Universities. He has over 15 years of academic experience in different reputed institutions of the world. He is currently an Associate Professor with the Department of Mathematics, Majmaah University, Saudi Arabia. He is also associated with Ton Duc Thang University, Vietnam, as a Researcher. He has published more than 250 research articles in different well-reputed international journals of the world. His expertise is in the areas of fluid dynamics, MHD flows, nanofluids, fractional derivatives, integral transforms, exact solutions, and mathematical modeling. He is the potential reviewer of many research journals of the world.

KOTTAKKARAN SOOPPY NISAR is currently an Associate Professor with the Department of Mathematics, Prince Sattam Bin Abdulaziz University, Saudi Arabia. He has more than 150 research publications. His current research interests include special functions, fractional calculus, and SAC-OCDMA code networks.